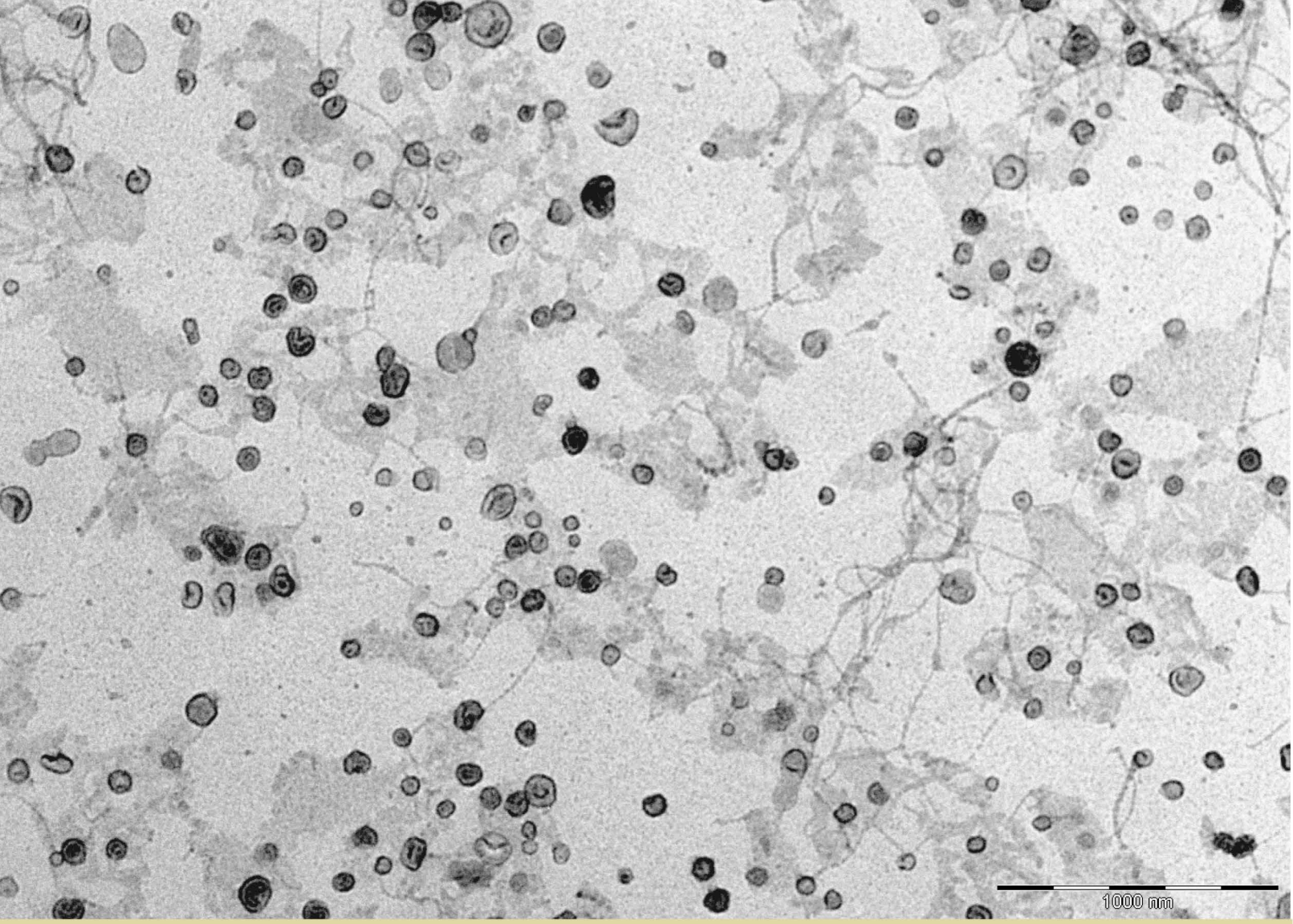

Carlos Alberto Gaspar de Jesus

Urine Extracellular Vesicles: Waste or a Powerful Tool?

Dissertação para a obtenção do grau de Mestre em Investigação Biomédica
sob orientação científica do Doutor Lino Ferreira e do Doutor Hugo Fernandes
e apresentada à Faculdade de Medicina da Universidade de Coimbra

Julho 2018

· U C ·

Universidade de Coimbra

Urine Extracellular Vesicles: Waste or a Powerful Tool?

Carlos Alberto Gaspar de Jesus

Dissertation for the attribution of the Master degree in Biomedical Research, submitted to the Faculty of Medicine of the University of Coimbra, Portugal. The experimental work described in this dissertation was performed at Center for Neuroscience and Cell Biology (CNC), in Biomaterials & Stem Cell-based Therapeutics Lab, in the unit UC-Biotech (Biocant Park), under the supervision of Doctor Lino Ferreira and Doctor Hugo Fernandes. This work had the collaboration of the cardiology department of the Centro Hospitalar e Universitário de Coimbra. This work was funded by FCT (MITP-TB/ECE/0013/2013), QREN-COMPETE funding (Project "StrokeTherapy" co-promoted by Stemlab, Rovisco Pais and Universidade de Coimbra) and European project ERAatUC (ref. 669088).

Dissertação para obtenção do grau de Mestre em Investigação Biomédica apresentada à Faculdade de Medicina da Universidade de Coimbra, Portugal. O trabalho experimental descrito nesta dissertação foi realizado no Centro de Neurociências e Biologia Celular (CNC), no grupo "Biomaterials & Stem Cell-based Therapeutics Lab", na unidade UC-Biotech (Biocant Park), sob a orientação científica do Doutor Lino Ferreira e do Doutor Hugo Fernandes. Este trabalho teve a colaboração do Departamento de Cardiologia do Centro Hospitalar e Universitário de Coimbra. Este projeto foi financiado pela FCT (MITP-TB/ECE/0013/2013), financiamento da QREN-COMPETE (Projeto "StrokeTherapy" em co-promoção com Stemlab, Rovisco Pais e Universidade de Coimbra) e pelo projeto Europeu ERAatUC (ref. 669088).

Coimbra, 2018

FACULDADE DE MEDICINA
UNIVERSIDADE D
COIMBRA

Front cover:

TEM image of extracellular vesicles isolated from a urine sample diluted in Tris-EDTA buffer. *Bar,* 1000 nm.

“Attitude is a little thing that

makes a big difference.”

Winston Churchill

Agradecimentos

Em primeiro lugar, quero agradecer ao Doutor Lino Ferreira e ao Doutor Hugo Fernandes pela oportunidade de fazer a tese neste grupo. Obrigado Doutor Hugo, por veres o meu potencial, pela paciência que tiveste e por me teres ajudado a crescer ao longo deste ano, tanto a nível pessoal como intelectual.

Agradecer ao Professor Fernando Mendes, que desde cedo viu em mim o gosto pelo curso e pela investigação e que sempre me aconselhou com base nos meus interesses.

Ao Professor Henrique Girão, pela maneira relaxada e animada com que sempre me recebe quando passo no seu laboratório. E como é óbvio, também ao resto dos g(u)ic.

Ao meu *sensei* Ricardo, por toda a tua paciência, disponibilidade e ensinamentos no laboratório. Conseguiste “contagiar” em mim o teu grande gosto pelos EVs. O facto de seres tão exigente contigo próprio fez com que eu também fosse exigente comigo. Ainda agradecer pelas boleias e pelas discussões interessantes sobre matérias distintas durante as viagens.

Ao “gangue dos mestrandos”: Cláudia, Raquel, Inês e Helena, pelos momentos de conversa e descontração. Com tanto mestrandos juntos, as conversas nunca podiam ser sérias.

Uma palavra de agradecimento ao resto dos E.T., foram incansáveis sempre que precisei de ajuda de algum de vós e sempre tentaram integrar-me no grupo.

Aos meus amigos mais próximos, principalmente ao Rui, Tatalo e Sara. Obrigado por se lembrarem de mim, pela paciência ao longo deste ano e pelos convites para cafés/jantares em que muitas vezes recusava porque estava a trabalhar. Mas em que outras situações não vos podia falhar.

A ti Kátia, por todo o carinho e conforto que me deste no último ano. Apareceste quando menos esperava, mas foste a melhor surpresa. Tu sabes o quanto significas para mim.

Resta agradecer à minha família porque “O amor da minha família é o maior presente que já recebi na vida!”. A ti mãe, por seres a mulher mais forte que conheço e por teres a força de me incentivar a seguir os caminhos que sabes que quero, mesmo quando isso implica que estejamos mais tempo sem nos ver. Ao meu pai e à minha avó, todas as decisões que tomo sinto que, de alguma forma, vocês me guiam. Aos meus irmãos Manuelito e António, cunhadas e sobrinhos que, mesmo longe, incentivam-me a lutar pelo que quero e mostram o quão importante e fortes são os nossos laços. Aos meus tios José e Gabriela, pelo carinho e orgulho que mostram ter por mim. E a ti prima Tânia, que sempre manténs o contato e perguntas quando volto para a Madeira.

Summary

According to the World Health Organization, ischemic heart disease is the leading cause of death worldwide with 17.7 million deaths in 2015. Acute myocardial infarction (AMI), an ischemic heart disease, is caused by the blockage of blood flow (nutrients and oxygen) to a specific area of the heart thus culminating in irreversible cell death and impaired cardiac function. The availability of diagnostic and therapeutic tools is still limited. Extracellular vesicles (EVs), small vesicles release by the cells, can be found in several biological fluids, such as blood, urine, breast milk, amongst others. Interestingly, they have been used for therapeutic and diagnosis purposes, inclusive in ischemic heart disease, with promising results.

The work herein described had two main aims: (i) isolate EVs from urine with high yield and purity and (ii) evaluate their bioactivity on endothelial cells (ECs).

Using an isolation protocol based on dilution of urine with Tris-EDTA (T-EDTA) we were able to isolate EVs with higher yield in 5 of 6 urine samples (ranging between 35% of decrease and 465% of increase) when compared to undiluted urine. Regarding the purity, upon dilution, we had an increase in all the samples, ranging from 178% and 969% when compared to undiluted urine. Furthermore, we characterized the obtained EVs using transmission electron microscopy, zeta potential, nanoparticle track analysis and flow cytometry.

Urine EVs from healthy donors and AMI patients were isolated and their bioactivity assessed on ECs. We showed that EVs from healthy donors only induced an increase on ECs proliferation whereas urine EVs from AMI patients induced an increase both in proliferation as well as migration of ECs, although in a donor dependent-manner.

Taking together, our results suggest that EVs from urine can be used as a therapeutic tool, in particular urine EVs derived from AMI patients.

Keywords: Acute myocardial infarction, extracellular vesicles, urine, Tamm-Horsfall protein, yield, purity, bioactivity assays, autologous therapy.

Sumário

De acordo com a Organização Mundial de Saúde (OMS), a cardiopatia isquémica é a principal causa de morte em todo o mundo, resultando em 17.7 milhões de mortes em 2015. O enfarte agudo do miocárdio (EAM), uma cardiopatia isquémica, é causado pelo bloqueio do fluxo sanguíneo (bloqueio de nutrientes e oxigénio) para uma área específica do coração, culminando em morte celular e num comprometimento da função cardíaca. A disponibilidade de ferramentas diagnósticas e terapêuticas ainda é limitada. Vesículas extracelulares (VEs), pequenas vesículas libertadas pelas células, podem ser encontradas em diversos fluídos, como o sangue, urine, leite materno, entre outros. Curiosamente, têm sido utilizadas para fins terapêuticos e diagnósticos, inclusive na cardiopatia isquémica, com resultados interessantes.

Este trabalho pode ser dividido em dois objetivos: (i) isolar VEs da urina com maior rendimento e pureza e (ii) avaliar a sua bioatividade em células endoteliais (CEs).

Utilizando um protocolo de isolamento baseado na diluição da urina com Tris-EDTA (T-EDTA) fomos capazes de isolar VEs com maior rendimento em 5 de 6 amostras de urina (variando entre 35% de redução e 465% de aumento) quando comparado à urina não diluída. Em relação à pureza, após diluição da urina, tivemos aumento em todas as amostras, variando entre 178% e 969% de aumento quando comparado à urina não diluída. Além disso, as VEs foram caraterizadas por microscopia eletrónica de transmissão, potencial zeta, *nanoparticle tracking analysis* e citometria de fluxo.

Nós usamos VEs da urina de dadores saudáveis e de pacientes com EAM em HUVECs para avaliar a sua bioatividade em CEs. Nós mostramos que as VEs de dadores saudáveis apenas induziram um aumento da proliferação de CEs, enquanto que as VEs da urina de pacientes com EAM induziram um aumento tanto da proliferação como da migração de CEs, no entanto, a intensidade do seu efeito foi dependente do dador.

Assim, os nossos resultados sugerem que VEs da urina podem ser utilizadas como uma ferramenta terapêutica, em especial as VEs isoladas de pacientes com EAM.

Palavras-Chave: Enfarte agudo do miocárdio, vesículas extracelulares, urina, proteína Tamm-Horsfall, eficiência, pureza, ensaio de bioatividade, terapia autóloga.

Index

Summary ..... *xi*

Sumário ..... *xiii*

Index ..... *xv*

Index of figures ..... *xix*

Index of tables ..... *xxi*

Glossary ..... *xxiii*

1. Introduction *1*

1.1. Cardiovascular diseases **1**

1.2. Acute myocardial infarction **2**

1.3. Extracellular vesicles **5**

1.3.1. Extracellular vesicles biogenesis and content 6

1.3.2. Translational potential of extracellular vesicles 7

1.3.3. Extracellular vesicles isolation methods 9

1.3.4. Extracellular vesicles in urine 10

2. Aims of the study *13*

3. Materials and Methods *15*

3.1. Urine sample collection **15**

3.2. Urine extracellular vesicle isolation optimization **15**

3.3. Characterization of urine extracellular vesicles **16**

3.3.1. Total protein quantification of urine extracellular vesicles 16

3.3.2. Zeta potential of urine extracellular vesicles 17

3.3.3. Size and concentration of urine extracellular vesicles 17

3.3.4. Transmission electron microscopy 18

3.3.5. Flow Cytometry 18

3.4. Cell culture and media 19

3.5. Media optimization for bioactivity assays 19

3.6. PrestoBlue™ measurement 20

3.7. Bioactivity assays 21

3.7.1. Proliferation assay 21

3.7.2. Survival assay 22

3.7.3. Migration assay 23

3.8. Cell fixation and nuclear staining 24

3.9. Image acquisition and analysis 24

3.10. Statistical analysis 24

3.11. Ethical Issues 24

4. Results 27

4.1. Optimization of urine EVs isolation 27

4.2. Characterization of urine EVs by flow cytometry 29

4.3. Characterization of EVs from urine by TEM 31

4.4. Cell media optimization for bioactivity assays 33

4.5. Bioactivity assays using EVs from urine of healthy donors 36

4.6. Bioactivity assays using EVs from urine of AMI patients 38

5. Discussion 43

6. Conclusion and further perspectives 51

7. References 53

8. Annex 65

8.1. Statistical analysis of "Cell media optimization for bioactivity assays" experiment 65

8.1.1. PrestoBlue™ measurement at 24 hours: 65

8.1.2. PrestoBlueTM measurement at 48 hours: 68

8.1.3. Cell number measurement at 48 hours:..... 71

8.1.4. Cell number vs PrestoPlueTM correlation at 48 hours..... 74

Index of figures

Figure 1 – Top 10 global causes of death in 2000 (A) and 2016 (B). 1

Figure 2 – Schematic representation of the interaction between endothelial cells and cardiomyocytes. 2

Figure 3 – Schematic representation of a myocardial injury due to blood flow interruption by a clot. 4

Figure 4 – Schematic representation of the three major classes of extracellular vesicles..... 7

Figure 5 – Different EVs isolation techniques based on their size, density or immunophenotype. 10

Figure 6 – Workflow for the urine collection of AMI patients upon arrival at the emergency service and subsequent days. 15

Figure 7 – Schematic representation of the urine EVs isolation optimization. . 16

Figure 8 – Experimental layout of the cell medium optimization for bioactivity assays. 20

Figure 9 – Schematic representation of the proliferation assay. 22

Figure 10 – Schematic representation of the survival assay. 23

Figure 11 – Schematic representation of the migration assay. 23

Figure 12 – T-EDTA dilution increases the yield and purity of urine EVs. 29

Figure 13 – Optimization of flow cytometry conditions using CD9 antibody. ... 30

Figure 14 – TEM analysis of urine EVs from donor 6. 32

Figure 15 – Cell media optimization for bioactivity assays using a proliferation assay in HUVECs. 35

Figure 16 – Bioactivity assays results using urine EVs from three healthy donors. 37

Figure 17 – Bioactivity assays results using urine EVs from two AMI patients. 40

Figure 18 – Schematic representation of the effect of T-EDTA dilution on THP found in urine..... 45

Index of tables

Table 1 – Expression of $CD9^+$, $CD63^+$ or $CD9^+CD63^+$ of EVs from T-EDTA diluted urine. 31

Table 2 – AMI patient donor data 49

Table 3 – Statistical analysis of PrestoBlue™ measurement at 24 hours. 65

Table 4 – Statistical analysis of PrestoBlue™ measurement at 48 hours. 68

Table 5 – Statistical analysis of cell number measurement at 48 hours. 71

Table 6 – Tabular results of the statistical analysis of the correlation between cell number and PrestoBlue™ results at 48 hours 74

Table 7 – XY data of the statistical analysis of the correlation between cell number and PrestoBlue™ results at 48 hours. 75

Glossary

Special characters

µg: Microgram;

µm: Micrometer;

A

AB: Apoptotic bodies;

AIDS: Acquired immune deficiency syndrome;

AMI: Acute myocardial infarction;

AQP2: Water channel aquaporin-2;

B

bFGF: Basic Fibroblast Growth Factor;

BSA: Bovine serum albumin;

C

CO_2: Carbon dioxide;

CD: Cluster of differentiation;

CHUC: Centro Hospitalar e Universitário de Coimbra;

CK-MB: Creatine kinase muscle-brain;

CMs: Cardiomyocytes;

cTn: Cardiac troponin;

cTnI: Cardiac troponin isoform I;

cTnT: Cardiac troponin isoform T;

CVDs: Cardiovascular diseases;

D

DMEM: Dulbecco's modified Eagle medium;

DTT: Dithiothreitol;

E

E: Endosome

EBM: Endothelial basal médium;

ECG: Electrocardiogram;

ECs: Endothelial cells;

EGF: Epidermal Growth Factor;

EGM-2: Endothelial cell growth medium 2;

EPCs: Endothelial progenitor cells;

ER: Emergency room;

EVs: Extracellular vesicles;

Ex: Exosomes;

F

FBS: Fetal bovine sérum;

FC: Flow cytometry;

G

GM-CSF: Granulocyte macrophage-colony stimulating factor;

H

HF: Heart failure;

hAECs: Human amniotic epithelial cells;

HEK293: Human embryonic kidney cells 293

hs-cTn: High-sensitive cardiac troponin;

HUVECs: Human umbilical vein endothelial cells;

I

IgG: Immunoglobulin G;

I/R: Ischemia/Reperfusion;

ILV: Intraluminal vesicles;

ISEV: International Society of Extracellular Vesicles;

L

L: Liter

LC-MS/MS: Nanospray liquid chromatography–tandem MS;

Long R3 IGF: Insulin-like Growth Factor;

M

MHC: Major histocompatibility complex;

microBCA: Micro bicinchoninic acid assay;

miRNA: MicroRNA;

mL: Milliliter;

mM: Millimolar;

mRNA: Messenger RNA;

MSCs: Mesenchymal stem cells;

mV: Millivolt;

MVB: Multivesicular body;

N

N: nucleus;

ng: Nanogram;

nm: Nanometers;

NO: Nitric Oxide;

NTA: Nanoparticle tracking analysis;

O

O_2: Oxygen;

P

PFA: Paraformaldehyde;

PALS: Phase analysis light scattering;

PBS: Phosphate buffered saline;

PEG: Polyethylene glycol;

PS: Penicillin/Streptomycin;

S

SAH: Systemic arterial hypertension;

SD: Standard deviation;

SDS: Sodium dodecyl sulphate;

SEC: Size exclusion chromatography;

T

T-EDTA: Tris-EDTA buffer;

TEM: Transmission electron microscopy;

THP: Tamm-Horsfall protein;

U

UC: Ultracentrifugation;

V

v/v: Volume/Volume percentage concentration;

VEGF: Vascular endothelial growth factor;

W

w/v: Weight/Volume percentage concentration;

WHO: World Health Organization.

1. Introduction

1.1. Cardiovascular diseases

In 2015, the World Health Organization (WHO) estimated that 17.7 million deaths were caused by cardiovascular diseases (CVDs), representing almost one-third of the Worldwide deaths. In fact, since the turn of the millennium, the two major causes of death worldwide have been ischemic heart disease and stroke, having more impact than respiratory infections, acquired immune deficiency syndrome (AIDS) or even cancer (figure 1A). Despite all the efforts and achievements in the cardiovascular field during the last decades, CVDs desperately need more and better diagnostic and therapeutic strategies (figure 1B) to mitigate their devastating effects.

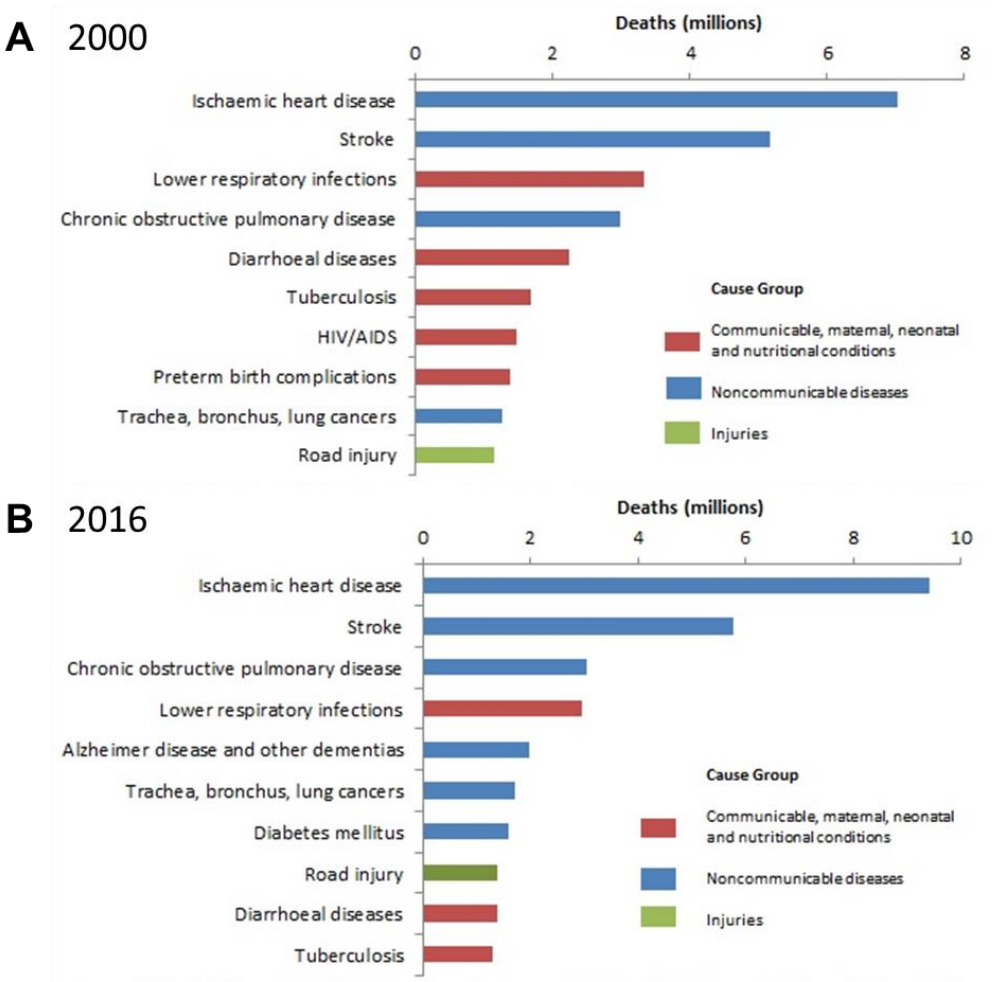

Figure 1 – Top 10 global causes of death in 2000 (**A**) and 2016 (**B**).

Source: World Health Organization (Adapted).

1.2. Acute myocardial infarction

Acute myocardial infarction (AMI), an ischemic heart disease, is caused by the blockage of blood flow (nutrients and oxygen) to a specific area of the heart thus culminating in irreversible cell death and loss of myocardial function[1,2]. After an AMI, the loss of cardiomyocytes (CMs) and endothelial cells (ECs) is, to some extent, ameliorated by the formation of scar tissue in the infarcted area due to the invasion and proliferation of fibroblasts[3]. In the adult, this is a natural wound healing process occurring in response to the death of the cardiac-specific cells and results in ventricular remodeling, a process characterized by changes in mass, volume and function of the left ventricle, eventually culminating in heart failure (HF)[3–5].

Around 2-4 billion of CMs form the bulk of the cardiac tissue and ultimately, they are responsible for the correct pumping of the blood from the heart to the rest of the body[5]. Despite accounting for 90% of the mass of the heart, CMs only represent around 30% of the total cell number. This is explained by the fact that each CM is surrounded by 3 or 4 capillaries[5,6]. ECs are, therefore, the most prevalent cell type in the normal heart, with an estimated ratio of 3 ECs to 1 CM, with direct and indirect interaction between them (figure 2)[7,8].

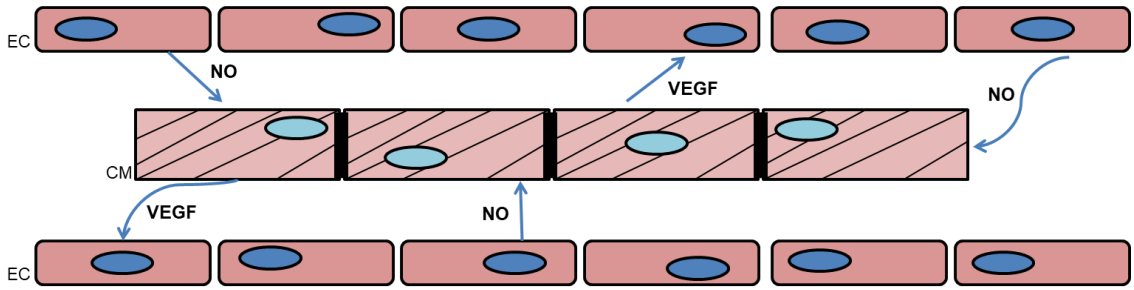

Figure 2 – Schematic representation of the interaction between endothelial cells and cardiomyocytes. Both cells can release molecules that will induce a response in the other cell type, such as survival (VEGF) or contraction (NO).

CM, cardiomyocytes; EC, endothelial cells; NO, nitric oxide; VEGF, vascular endothelial growth factor.

Upon heart injury, endothelial progenitors cells (EPCs) are recruited from the bone-marrow to the circulation in an attempt to restore the homeostatic state by forming new blood vessels[5,8–10], a mechanism denominated

angiogenesis. Takahashi *et al.* have showed that the injection of EPCs into mice with hindlimb ischemia resulted in their incorporation into the ischemic lesion and *in situ* differentiation into ECs[9]. Interestingly, using another animal model, they showed that a pretreatment of rabbits with granulocyte macrophage-colony stimulating factor (GM-CSF) increased the EPC-enriched cell population, enhanced EPCs differentiation into ECs and increased angiogenesis after hindlimb ischemia when compared to control group[9].

Angiogenesis is an attractive therapeutic target that can be modulated, between others, by several microRNAs[11–13] and molecules, such as miRNA-126[14] and vascular endothelial growth factor (VEGF)[8], respectively. Upon ischemic heart injury, cardiac cells are exposed to an hostile environment comprising low levels of oxygen which in turn induce the activation of the hypoxia signaling pathway, ultimately culminating in recruitment of EPCs and formation of new blood vessels[15]. This process is orchestrated by the proliferation, sprouting and migration of ECs[13].

After confirming the diagnosis of AMI, the first intervention performed by the medical team consists on the reperfusion of the damaged myocardium thus restoring the blood supply to the area downstream of the blockage. However, the reperfusion of the damaged myocardium further exacerbates the injury, a process denominated Ischemia/Reperfusion (I/R) damage[16,17]. This I/R damage is due to the increase of superoxide anion radicals, induction of inflammatory response and inhibition of the endogenous anti-oxidant mechanisms[18]. The prognosis of the patient will depend on the extension of the I/R damage since this will directly affect the infarct size, left ventricular function and remodeling[3,17].

Patients that suffered an ischemic heart event often develop HF which will reduce their quality of life and, more worryingly, has a 5-year mortality close to 50%[19]. Diverse strategies are used to relieve HF symptoms and increase patient´s quality of life such as cardiac devices[20,21], beta blockers[22], aldosterone antagonists[23] and angiotensin-converting-enzyme inhibitors[23,24]. Unfortunately, there is no “cure” and the only way to overcome HF is heart transplant, a highly risky and costly medical procedure. Consequently, disease prevention and early diagnostic of cardiovascular events remains the most effective options. For the diagnostic of AMI several complementary techniques are available such as the

identification of particular biomarkers, electrocardiogram (ECG) and heart imaging[1,2].

Upon cell death due to AMI, the affected cardiac cells release their intracellular content (proteins, metabolites and extracellular vesicles [EVs]) and these can be used as biomarkers of myocardial injury (figure 3)[25–27]. Several biomarkers for AMI can be used but the most reliable biomarker is cardiac troponin (cTn)[1,2,25,26]. cTns are important for the contractibility of the heart and the isoforms I (cTnI) and T (cTnT) are not expressed in any organ other than the heart, making them specific biomarkers for myocardial injury[28,29]. Recently, high-sensitive cTn (hs-cTn) have been developed and introduced into the laboratory routine improving the ability to detect much lower levels of cTns in a shorter time[30,31]. According to guidelines for AMI diagnosis, cTns needs to be above the 99th percentile of a reference population and a rise or fall of cTns levels need to be detected in order to confirm the diagnostic[2,32]. The reference values for hs-cTnI adopted at the cardiology department of the Centro Hospitalar e Universitário de Coimbra are under 34 ng/mL and 16 ng/mL for men and women, respectively.

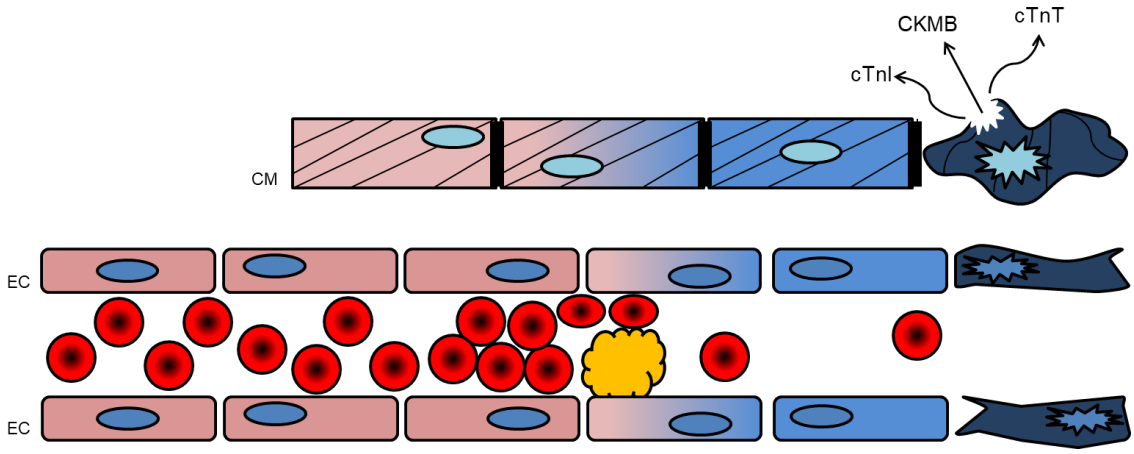

Figure 3 – Schematic representation of a myocardial injury due to blood flow interruption by a clot. Downstream of the blockage, cardiac cells start to die due to the lack of oxygen and nutrients, releasing their content. The factors released by dead cells can be exploited as biomarkers of myocardial injury.

CM, cardiomyocytes; EC, endothelial cells; cTnI, cardiac troponin I; cTnT, cardiac troponin T; CKMB, creatine kinase muscle-brain.

However, an increase in cTns can be found in individuals without myocardial necrosis such as, for example, in healthy high-performance athletes or even after rapid atrial pacing. Moreover, cTns cannot be used to distinguish the type of CVD such as, for example, coronary artery disease and unstable angina[25]. Therefore, the use of biomarkers such as cTns for diagnosing myocardial injury needs to be carefully interpreted and preferentially supported with ECG and heart imaging[1,2,25,33].

Besides the use of cTns, EVs have been described as potential biomarkers for cardiac injury[27]. In fact, Deddens *et al.* have showed in a porcine animal model that EVs are released from the damaged myocardium after I/R injury. They were able to show that the expression of heart-specific microRNAs (miR-1, miR-133b, miR-208b and miR-499) was increased between 200 and 800 fold on EVs after heart attack[27]. However, more research in this field is required to unravel the potential of these vesicles.

Altogether, the diagnosis and treatment of AMI is still challenging and more, better and cheaper prognostic, diagnostic and therapeutic tools are desperately needed in order to overcome this major problem. In the last decades, an increasing interest in the theranostic potential of EVs has emerged since these have a great potential as both biomarkers and therapeutics tools in different health areas.

1.3. Extracellular vesicles

Since the 80's it is known that the maturation of sheep or rat reticulocytes into erythrocytes is mediated by the release of transferrin receptors by vesicles[34,35]. Back then, it was believed that these vesicles, originated from a cellular secretory pathway, were responsible for the clearance of detrimental components of the plasma membrane[34–36]. In 1987, Johnstone *et al.* showed that the release of this vesicles resulted from the fusion of multivesicular bodies (MVBs) with the plasma membrane and, for the first time, the term "exosomes" was used[36]. Then, Raposo *et al.* and Zitvogel *et al.* reported the release of similar vesicles, of endosomal origin, in B lymphocytes and dendritic cells[37,38]. Finally, in 2007, Valadi *et al.* showed that exosomes can

transport functional nucleic acids, opening a new world of opportunities and increasing the interest on this emerging field[39]. Nowadays, vesicles released by cells are called extracellular vesicles (EVs), in order to encompass apoptotic bodies, microvesicles and exosomes into the family of vesicles secreted by cells[40,41].

1.3.1. Extracellular vesicles biogenesis and content

According to their size and secretion pathway, EVs can be classified into 3 major groups: apoptotic bodies, microvesicles and exosomes (figure 4)[42–44]. Apoptotic bodies (AB) originate from programmed cell death and have a diameter between 1000 and 5000 nm. It has been shown that AB can carry DNA, RNA and histone proteins, between others, and they have the ability to present their content to macrophages in order to be phagocytized (figure 4c)[42,44–46]. Microvesicles are intermediate to large size vesicles with a diameter between 150 and 1000 nm[47,48]. These vesicles result from direct plasma membrane outward budding, playing an important role in wound recovery of plasma membranes (figure 4b)[44,47–50]. Finally, exosomes are the smallest vesicles produced by cells, ranging in diameter between 30 and 200 nm[51]. Exosomes result from the invagination of endosomes, producing intraluminal vesicles (ILV) and giving rise to MVB which, upon fusion with the plasma membrane, release exosomes to the extracellular space (figure 4a)[40,52–55].

All these vesicles can transport diverse molecules for intercellular communication, such as proteins, lipids and nucleic acids, including microRNAs (miRNAs). miRNAs are small RNA molecules of 18 to 25 nucleotides that have the ability to bind to complementary sequences in target messenger RNA (mRNA), thereby mediating its degradation or blocking its translation, resulting in inhibition of protein production[56–59]. miRNAs are important players in intracellular signaling since one single miRNA can bind to different mRNAs thus modulating several different pathways simultaneously[56–58].

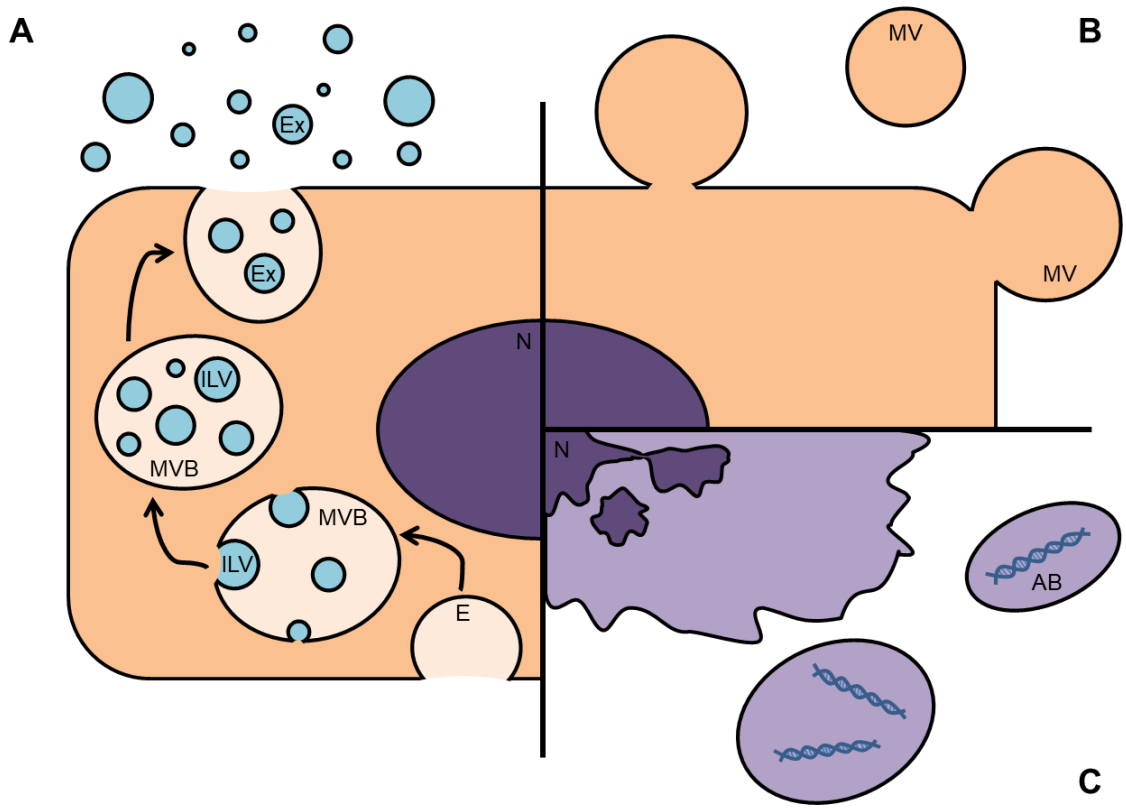

Figure 4 – Schematic representation of the three major classes of extracellular vesicles. **A)** Exosome biogenesis starts with the invagination of the endosome, resulting in the formation of a MVB that will fuse with the plasma membrane, releasing the exosomes. **B)** Membrane outward budding resulting in microvesicle release. **C)** Apoptotic body release by an apoptotic cell.

E, endosome; MVB, multivesicular body; ILV, intraluminal vesicle; Ex, exosomes; MV, microvesicle; AB, apoptotic body; N, Nucleus.

1.3.2. Translational potential of extracellular vesicles

Since the discovery of the existence of miRNAs and mRNA inside EVs by Valadi *et al.*[39], EVs have gathered great interest not only in the academia/research field but also in the corporate field. Their seminal work led to the creation of Codiak BioSciences, a company that is “Realizing the potential of exosome biology” by developing bioengineered exosomes. In total, there are only 14 EVs-related companies worldwide, one of them a Portuguese (Exogenus Therapeutics). Established cell-based companies, such as Lonza, have also showed their interest in investing in this exciting field clearly showing

the potential of EVs in translational research/technology both for diagnostic as well as for therapy.

EVs are important not only in physiologic conditions but also in disease. For example, it is known that cancer cells produce significantly more EVs than healthy cells[60,61]. Some cells can produce EVs in which their natural content can induce therapeutic response, such as mesenchymal stem cells (MSC)[62,63]. One of the biggest success cases using EVs was reported for the treatment of a patient with graft-versus-host disease[64]. In this study, one patient was injected every 2-3 days with MSCs EVs starting with a low quantity of EVs (0.1 unit) and increasing the dose in every next injection (until it reached 4 units). One unit was considered as “the yield of an EV fraction prepared from supernatants of 4 x 10^7 MSCs that had been conditioned for 48 hours”[64]. Within 2 weeks of the EVs treatment, patient’s cutaneous and mucosal improved remarkably, remaining stable even after 4 months since the treatment[64].

Another way to use EVs as a therapeutic agent is by engineering EVs content. This approach is getting popular since it is give the researcher the possibility to incorporate onto EVs a selected molecule, such as miRNAs or drugs, adapting those EVs for a given therapeutic indication[65–70]. Kim *et al.* loaded EVs with paclitaxel, a well-known anticancer drug, and using a multi-drug resistant cell line, they were able to show that the paclitaxel-loaded EVs led to a 50 fold increase in cytotoxicity compared with paclitaxel alone[70]. In fact, they used these paclitaxel-loaded EVs in a model of murine Lewis Lung Carcinoma pulmonary metastases and showed a potent anticancer effect when compared with both taxol alone or control EVs[70].

Beyond the therapeutic potential, EVs are often used for diagnosis, such as in cancer[71–73], kidney disease[74,75], heart diseases[27,76], amongst others[77–79]. For example, miR-141 and miR-375 were found to be over-expressed in serum EVs from patients with recurrent disease after the removal of prostate cancer when compare with patients without recurrent disease[80]. Moreover, circulating miR-141 alone can be used as a biomarker for prostate cancer[81]. Based on these evidences, many researchers are using proteomics and genomics to identify within the EVs novel biomarkers for a given disease.

1.3.3. Extracellular vesicles isolation methods

EVs can be isolated from several biofluids using by diverse isolation methods[82,83]. The isolation method most often used is differential ultracentrifugation (figure 5A)[36,37,82–86]. Differential ultracentrifugation consists in submitting the sample to sequential centrifugations at different speeds to isolate different types of vesicles. Generally, the sample is centrifuged at low speed (300 g) to remove cells, then at 2.000 g to remove apoptotic bodies and cell debris, at 10.000 g to remove large vesicles and finally, to pellet mostly exosomes, the sample is centrifuge at 100.000 g[36,37,82–87]. It is recommended to perform a purification step after isolation of EVs based on differential centrifugation by subjecting the obtained sample to a density gradient centrifugation (figure 5B). Using density gradient centrifugation, it will be possible to separate the vesicles by size but also by density, increasing the purity of the EV preparation[41,83,86–88]. Differential ultracentrifugation will pellet EVs but also contaminants with different densities, such as protein aggregates and cholesterol, amongst others and again, a subsequent density gradient centrifugation is warranted to increase the purity.

Another widely used method is size exclusion chromatography (SEC) in which particles pass through a gel with a given pore size and particles are filtered based on their size, wherein small particles migrate slower (they are entrapped in the pore) than bigger particles (figure 5C)[82,83,87,89]. Another method that separates EVs based on their size is the ultrafiltration, a method where the sample passes through membrane filters with different sizes (figure 5D). The last filter will have the adequate size for the targeted EVs[82,83,87,90,91].

An alternative method for EVs isolation is immunoaffinity-based isolation technique (figure 5E)[82,83,87]. In this method, the sample containing EVs is isolated based on their immunophenotyped upon incubation of EVs with monoclonal antibodies against classical EV surface markers[82,83,87,92].

The last of the most well-known EVs isolation methods is hydrophilic polymer precipitation methods (figure 5F)[82,83,87]. This simple method consists in decreasing the solubility of the EVs in the solution using hydrophilic polymers, such as PEG, thus allowing the precipitation of EVs using low-speed benchtop centrifugation[82,83,87,93].

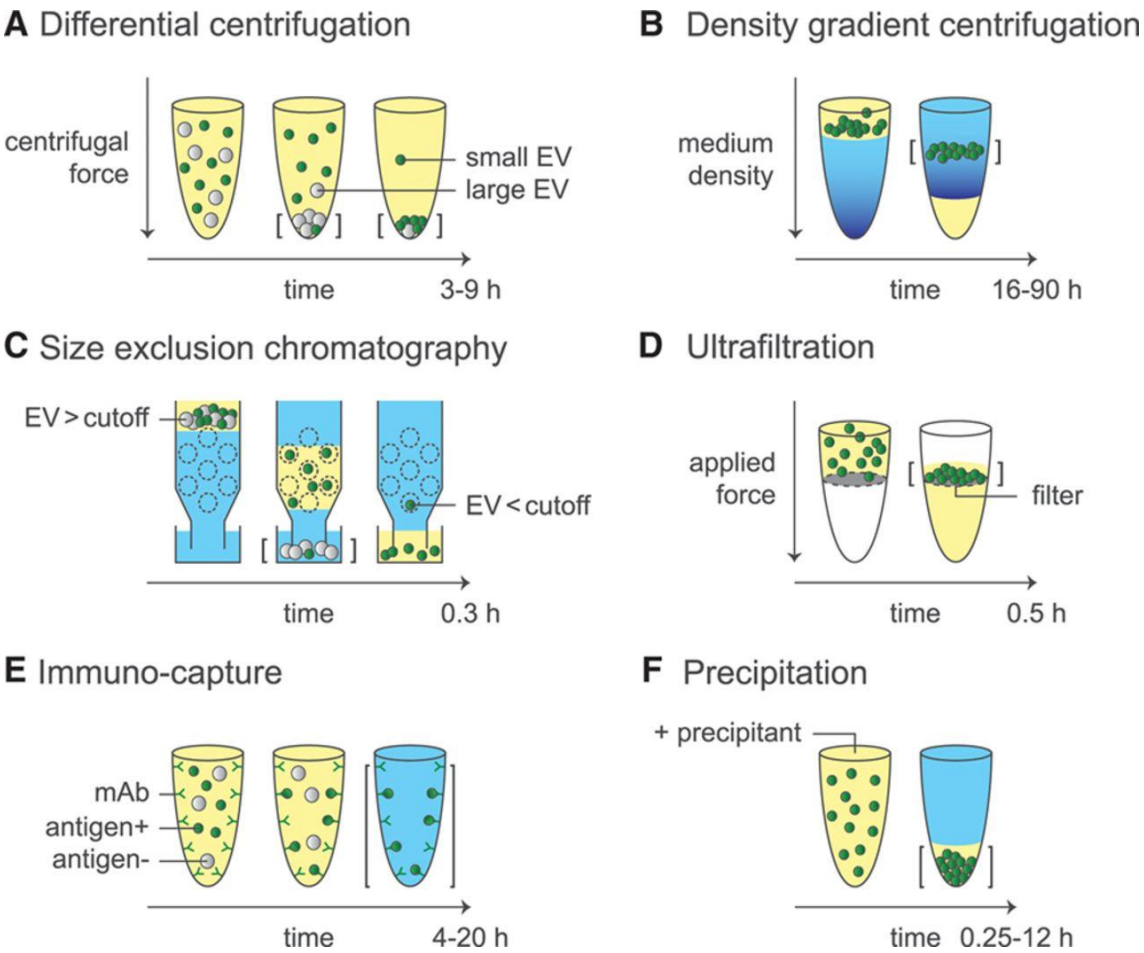

Figure 5 – Different EVs isolation techniques based on their size, density or immunophenotype. **A)** EVs isolation using differential ultracentrifugation; **B)** Purification of EVs by density gradient ultracentrifugation; **C)** EVs isolation method by size exclusion chromatography; **D)** Isolation of EVs by ultrafiltration; **E)** Immuno-capture of EVs based on their immunophenotype properties; **F)** EVs isolation using hydrophilic polymer precipitation methods, such as PEG.

Figure from: "Methodological Guidelines to Study Extracellular Vesicles"; Coumans *et al.*; 2017.

1.3.4. Extracellular vesicles in urine

EVs can be released virtually by all the cells of the organism and can be found in numerous body fluids, such as blood, urine, saliva, breast milk, among others[40,94–98].

Compared with other EV sources, urine has many important advantages since it can be collected non-invasively and in large amounts. Moreover, urine is already used as a biofluid for biomarker discovery[99]. It is known that urine contains large amounts of EVs and that it may transport

biomolecules that can convey information about renal and urological function[100–102]. The first report regarding isolation of EVs from urine dates back to 2004 when Pisitkun *et al.*[103] showed, by immunogold electron microscopy, that the water channel aquaporin-2 (AQP2), a biomarker related with many water-balance disorders, is excreted through EVs. They hypothesized that urine EVs could be used to identify renal diseases biomarkers and, using nanospray liquid chromatography–tandem MS (LC–MS/MS) of urine EVs, they showed the presence of 21 proteins related with renal diseases or blood pressure regulation[103].

Despite the many advantages of urine as a source of EVs one must also consider some potential limitations[99]. Tamm-Horsfall protein (THP) is the most abundant protein found in human urine[99,104]. Given the presence of cations such as Ca^{2+} and Na^{+} ions and an acidic pH, this filamentous protein tends to aggregate in networks or gel-matrices, resulting in the entrapment of EVs and their elimination in the first steps of low-speed centrifugations[99,105–107]. In order to disrupt these THP aggregates, the urine sample can be pretreated with a reducing agent called dithiothreitol (DTT)[103,107]. However, the EV yield using DTT has not been quantified and it adds extra steps to an already long isolation protocol[99].

Recently, Puhka *et al.* developed a simple protocol capable of increasing the yield of EVs from urine[99]. Urine samples were diluted in Tris-HCl (20 mM) buffer or Tris-HCl (20 mM) plus EDTA (20 mM) buffer at different pH (8.6 or 9), isolated by ultracentrifugation and the presence of classical EV markers and potential contaminants was assessed by western blot. Using this method, the authors showed that the dilution with Tris-HCL plus EDTA increased the yield of EVs between 2-7 fold, when compared to undiluted control, without affecting their morphology[99].

Although urine EVs are more often used to study renal and urological function[100–103], recent reports suggest that they can be used to identify biomarkers related with other diseases such as, for example, cardiac-related diseases[108]. In fact, Cheng *et al.* performed an interesting experiment demonstrating that systemic EVs can be eliminated by the kidney[108]. The authors collected EVs from serum of rats after AMI and injected them into rats

without AMI. They were able to see an increase in the heart-enriched miRNA-1 in the urine after 3 to 6 hours of the injection. To further confirm that circulating EVs could reach the urine they decided to label EVs with a fluorescent dye and then injected them into the circulating blood of rats. After 12 hours, they collected the urine of these rats, isolated the EVs by ultracentrifugation and added the EVs to HEK293 cells. After incubation, they visualized that the cells had the fluorescence-labeled EVs suggesting that blood EVs can be filtered by the kidney and be found in the urine excreted by the animal[108].

2. Aims of the study

EVs are important in intercellular-communication in both health and disease, being promising players. Urine can be used as a source of EVs for diagnostic and therapeutic applications providing that some limitations are overcome.

The main goal of this work is to is to: (i) isolate EVs from urine with high yield and purity and (ii) evaluate their bioactivity on endothelial cells (ECs).

3. Materials and Methods

3.1. Urine sample collection

Urine samples from healthy donors and from AMI patients were collected upon informed consent was obtained. Between 50 mL and 150 mL of urine samples were collected into urine sample containers and stored at -80 ºC. Only one sample was collected from 6 healthy donors (3 males and 3 females). Two patients that suffered AMI entered in this study. Urine collection of those patients consisted in three collections for each patient at different time points: 1) <6 hours after admission of the patient into the emergency service, 2) in the day 2 of the patient hospitalization and 3) in the day 3 of the patient hospitalization (figure 6).

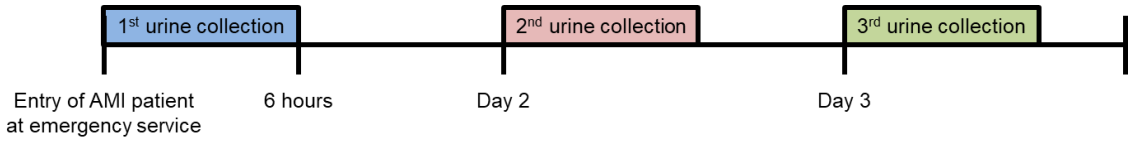

Figure 6 – Workflow for the urine collection of AMI patients upon arrival at the emergency service and subsequent days.

3.2. Urine extracellular vesicle isolation optimization

Optimization of EV isolation from urine was based on the protocol described by Puhka *et al.*[99]. Samples from 6 healthy donors (3 males and 3 females) were used to this end. Briefly, samples were thawed 15 minutes at 37 ºC, vortexed for 90 seconds at 2.500 rpm and centrifuged for 20 minutes at 2.000 g and 4 ºC to pellet cells and cell debris. Upon centrifugation, the supernatant was diluted 4 times (7 mL of urine supernatant with 21 mL of the dilution solution) in phosphate buffered saline (PBS), Tris-EDTA (20 mM, pH 9.0) or no dilution was performed (28 mL of urine supernatant). Regardless of the dilution agent, all samples were vortexed 90 seconds at 2.500 rpm to disrupt THP aggregates. In order to remove large vesicles from the preparation, the diluted samples were ultracentrifuged twice at 10.000 g for 30 minutes at 4 ºC. The resulting supernatant was submitted to an ultracentrifugation at 100.000 g for 2 hours at 4 ºC, to pellet small EVs (mainly exosomes). Finally, the pellet from the last step was washed with cold PBS, ultracentrifuged again at 100.000

g for 2 hours at 4 ºC, resuspended in 150 µL of cold PBS and conserved at -80 ºC for further characterization (figure 7). Ultracentrifugation steps were performed using a swinging bucket rotor SW 32 Ti in an Optima™ XPN 100K ultracentrifuge (Beckman Coulter, California, U.S.A.) and 28.7 mL polyallomer conical tubes (Beckman Coulter).

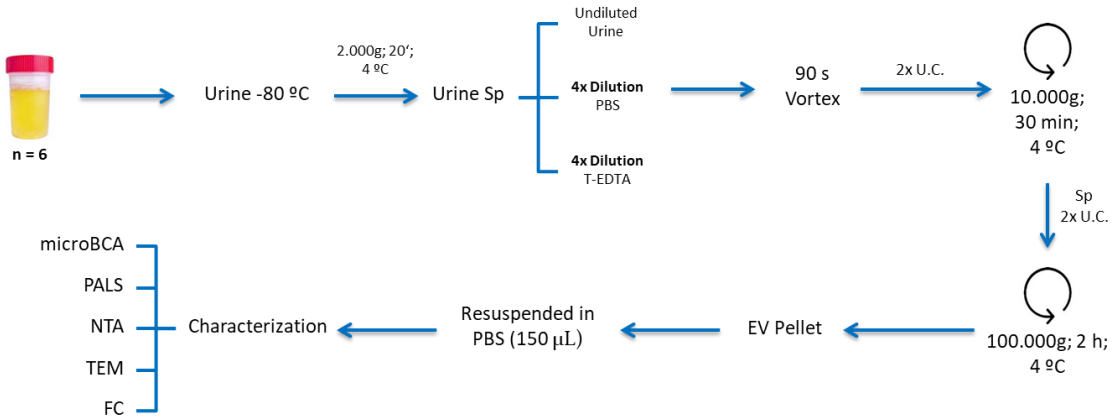

Figure 7 – Schematic representation of the urine EVs isolation optimization.

microBCA™, micro bicinchoninic acid assay; PALS, phase analysis light scattering; NTA, nanoparticle tracking analysis; TEM, transmission electron microscopy; FC, flow cytometry

3.3. Characterization of urine extracellular vesicles

To characterize the biophysical properties of the urine extracellular vesicles several techniques were employed. The micro bicinchoninic acid assay (microBCA™) was used to quantify the total amount of protein, phase analysis light scattering (PALS) was used to quantify the particle surface charge by zeta potential, nanoparticle tracking analysis (NTA) was used to quantify the particle size and concentration, transmission electron microscopy (TEM) was used to analyze the purity and EV morphology and flow cytometry (FC) was used to analyze the expression of typical EV markers.

3.3.1. Total protein quantification of urine extracellular vesicles

For total protein quantification of urine EVs microBCA™ protein assay kit (Thermo Fisher Scientific, Massachusetts, U.S.A.) was used following manufacturer's recommendations. Briefly, bovine serum albumin (BSA) was used to obtain a standard curve and 5 µL of EVs in PBS were diluted in 105 µL

of 2% (v/v) sodium dodecyl sulphate (SDS) to disrupt EV membrane. Then, 50 µL of the previous mix were pipetted in duplicate into a 96-well Corning® Costar® cell culture plates (Corning Inc., New York, U.S.A.). Commercial reaction solution was added and incubated for 2 hours at 37 ºC. Subsequently, the plates were equilibrated at room temperature for 15 minutes and the absorbance at 562 nm was read in the microplate reader Synergy™ H1 (Biotek, Vermont, U.S.A.).

3.3.2. Zeta potential of urine extracellular vesicles

NanoBrook ZetaPALS Potential Analyzer (Brookhaven Instruments Corporation, Long Island, U.S.A.) was used for urine EVs surface charge measurement. Briefly, 5 µL of urine EVs in PBS were diluted in 1500 µL of biological grade ultrapure water (Fisher Scientific, New Hampshire, U.S.A.), filtered twice through a 0.2 µM filter and the suspension was placed in contact with the zeta potential electrode. Five runs (using Smoluchowski module) were performed for each sample at room temperature.

3.3.3. Size and concentration of urine extracellular vesicles

Size and concentration of urine EVs was obtained using NTA using a NanoSight NS300 (Malvern Instruments, Malvern, U.K.). Urine EVs were diluted in PBS until a concentration between 15 and 45 particles/frame was obtained. The PBS used was confirmed to be pure (<5 particles per frame). For each sample, 5 videos of 30 seconds were recorded with the camera level set at 13. All the videos were processed with NTA 3.0 analytical software, using the software threshold between 2 and 4 depending on the quality of the videos, as described in the literature[109]. All the events with high size and low intensity (>200 nm and <0.5 of intensity) or low size and high intensity (<100 nm and >0.5 of intensity) were considered artefacts and removed from the analysis as per manufacturer's instructions. The application of these criteria led to the exclusion of less than 15% of the total number of events measured.

3.3.4. Transmission electron microscopy

Transmission electron microscopy (TEM) of EVs from urine diluted with Tris-EDTA or non-diluted was performed as described by Théry *et al.*[86]. Briefly, EVs were mixed with 4% (v/v) PFA 1:1 (v/v) to a final concentration of 2% (v/v) of PFA and deposited on Formvar-carbon coated grids (TAAB Technologies) for 20 min at room temperature. After washing 4 times with PBS, grids were placed on a drop of 1% (v/v) glutaraldehyde for 5 min, followed by washes with distilled water. In a dark environment, grids were incubated with uranyl-oxalate solution pH=7 for 5 min, and then placed on ice in contact with a solution of methyl cellulose (9:1) for 10 min. EV imaging was obtained using a Tecnai G2 Spirit BioTWIN electron microscope (FEI) at 80 kV. EV size from TEM images was calculated using the open-source image processing software Fiji/ImageJ.

3.3.5. Flow Cytometry

Flow cytometry (FC) was used to analyse the expression of classical EV surface markers CD9 and CD63. A few modifications were introduced to the protocol reported by Théry *et al.*[86]. In brief, different concentrations of EVs from undiluted or Tris-EDTA diluted urine (5.0×10^9, 1.0×10^{10}, 2.5×10^{10} or 5.0×10^{10} particles) were incubated with 5 µL of 3.8 µm aldehyde/sulfate latex beads (Life Technologies, California, U.S.A., catalog number: A37304) for 15 minutes. Then, PBS was added to a final volume of 1 mL and the solution was incubated overnight at 4 ºC with constant mixing, to promote EV adsorption to the beads. On the following day, in order to saturate all the beads free binding sites, 110 µL of 1 M glycine was added and incubated for 30 minutes at room temperature. Then, the suspension was centrifuged at 1.300 g for 3 minutes and the pelleted beads were resuspended and washed three times using 1 mL of 0.5% (w/v) BSA/PBS. After the washing steps, beads were resuspended in 0.5% (w/v) BSA/PBS and aliquoted in 150 µL aliquots to perform the antibody staining. To that end, 5 µL of antibody (see details below) was added to 150 µL of bead-bound EVs, incubated for 30 minutes at 4 ºC and washed twice as described before. Finally, the supernatant was discarded, the bead-bound EVs were resuspended in 100 µL of 0.5% (w/v) BSA/PBS and the analysis was performed

using a BD Accuri 6 (BD Bioscience, New Jersey, U.S.A.). The data was analyzed using Flowjo™ (v10, FlowJo, LLC).

The following commercially available antibodies were used: CD9-FITC (R&D Systems, Minnesota, U.S.A., catalog number: FAB1880F), CD63-PE (Invitrogen, California, U.S.A., catalog number: 12-063942), mouse IgG2B isotype control (R&D Systems, catalog number: IC0041F), mouse IgG_1 isotype control (R&D Systems, catalog number: IC002P).

3.4. Cell culture and media

Human umbilical vein endothelial cells (HUVECs; Lonza, Basel, Switzerland) between passage 3 and 6 were seeded onto 1% (w/v) porcine skin type A gelatin-coated flasks in endothelial cell growth medium 2 (EGM-2; PromoCell, Heidelberg, Germany) at 37 ºC, 5% of CO_2. EGM-2 was reconstituted as per manufacturer's recommendations with the addition of all the factors, 2% (v/v) of fetal bovine serum (FBS) and 0.5% (v/v) of Penicillin/Streptomycin (PS) into the endothelial basal medium (EBM). Starvation media for cell cycle synchronization consisted of EBM with 0.1% (v/v) of FBS. To avoid any confounding effect from bovine-derived EVs, all the medium used in our experiments was previously subjected to a FBS-EV depletion step. To that end, EBM with the required percentage of FBS was ultracentrifuged at 100.000 g for 18 hours and only the supernatant was used for further experiments. Importantly, when EGM-2 EV-depleted media was required, all the factors were added to the media only after the EV depletion was performed since growth factors and proteins can precipitate during the ultracentrifugation.

3.5. Media optimization for bioactivity assays

Our group has previous experience with bioactivity assays in ECs. However, during the course of the experiments, we had to change the endothelial media provider due to technical reasons. Thus, to optimize the new medium, we decided to use the classical endothelial proliferation assay.

In brief, 5.000 HUVECs were plated onto 96-well Corning® Costar® cell culture plates (Corning Inc.) and left to adhere overnight. In the next day, the medium was carefully discarded and EBM containing different concentrations of FBS (0%, 0.1%, 1%, 2%, 5% and 10% (v/v)) was added to the cells either alone or supplemented with 50 ng/mL of VEGF. EGM-2 medium was used as a control. After 24 hours of incubation with the different media, PrestoBlue™ Cell Viability Reagent (Thermo Fisher Scientific) was used to assess cell metabolism as per manufacturer´s instructions (see details below). Subsequently, PrestoBlue™ was discarded, new media was added and cells were incubated for further 24 hours. After this extra 24 hours we performed the PrestoBlue™ assay again (48 hour time point). After obtaining the results, the medium was discarded, cells were washed with PBS, fixed with 4% (v/v) PFA, the cell nuclei was stained with 10 ng/mL of Hoechst and nuclear counts were obtained using a high-content image microscope (see details below in chapter 3.8 and 3.9) (InCell Analyzer 2200; GE Healthcare, Little Chalfont, U.K.). For this experiment, 7 replicates were performed per condition. Resume of this experiment is represented in figure 8.

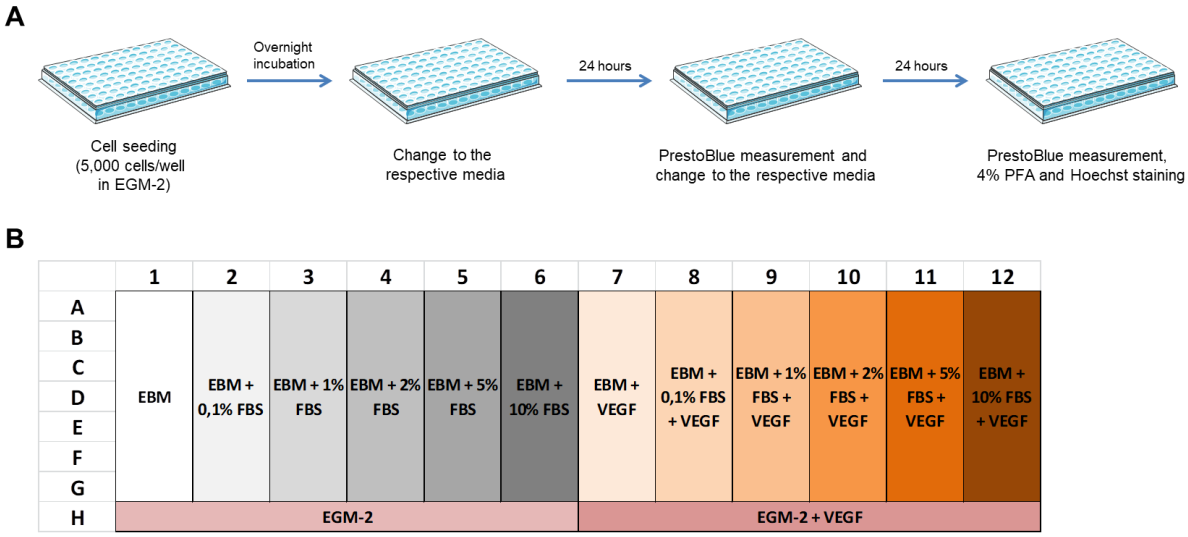

Figure 8 – Experimental layout of the cell medium optimization for bioactivity assays. **A)** Workflow of the experiment. **B)** Layout of the experimental conditions tested (n=7).

3.6. PrestoBlue™ measurement

For cell viability and metabolism evaluation, PrestoBlue™ Cell Viability Reagent (Thermo Fisher Scientific) was used as manufacturer's

recommendations. Briefly, PrestoBlue™ reagent was diluted 10 times in EGM-2 and the solution was equilibrated at 37 ºC prior to addition to the cells. Subsequently, cells were incubated for 1 to 2 hours at 37 ºC and 5% of CO_2 upon which, 80 uL of solution was transferred to 96-well Corning® Costar® black assay plate and fluorescence was measured (excitation: 560nm; emission: 590 nm) using the microplate reader Synergy™ H1 (Biotek). EGM-2 plus PrestoBlue™ reagent was used as a blank.

3.7. Bioactivity assays

In order to analyse the therapeutic potential of urine EVs, three different bioactivity assays using ECs (HUVECs) were performed: proliferation, survival and migration. HUVECS between passage 4 and 6 were incubated for 24 hours in FBS-EV depleted EGM-2 with 3 different concentrations (1.5×10^9, 3.0×10^9 and 4.5×10^9 particles/mL) of urine EVs from healthy donors and AMI patients. As positive controls, FBS-EV depleted EGM-2 and 50 ng/mL of VEGF were used. In the condition where VEGF was used, fresh VEGF was added every time that the medium was changed. In each assay, 5 replicates were performed per condition.

3.7.1. Proliferation assay

Briefly, 2.500 HUVECs per well were plated in 96-well Corning® Costar® cell culture plates in EGM-2 medium and left to adhere for 4 to 6 hours. Then, the medium was changed to starvation media for 12 to 16h (EBM supplemented with 0.1% (v/v) FBS) in order to synchronize the cell cycle. In the next day, the medium was discarded and FBS-EV depleted EGM-2 medium containing EVs or VEGF was added to the cells and incubated for 24 hours at 37ºC and 5% of CO_2. After the 24 hours of incubation, the media was discarded and FBS-EV depleted EBM supplemented with 5% (v/v) of FBS was added to the cells and incubated for 48 hours. Lastly, the medium was discarded, cells were washed with PBS, fixed with PFA, the cell nuclei was stained and nuclear counts were obtained using a high-content image microscope (see details below in chapter 3.8 and 3.9) (figure 9).

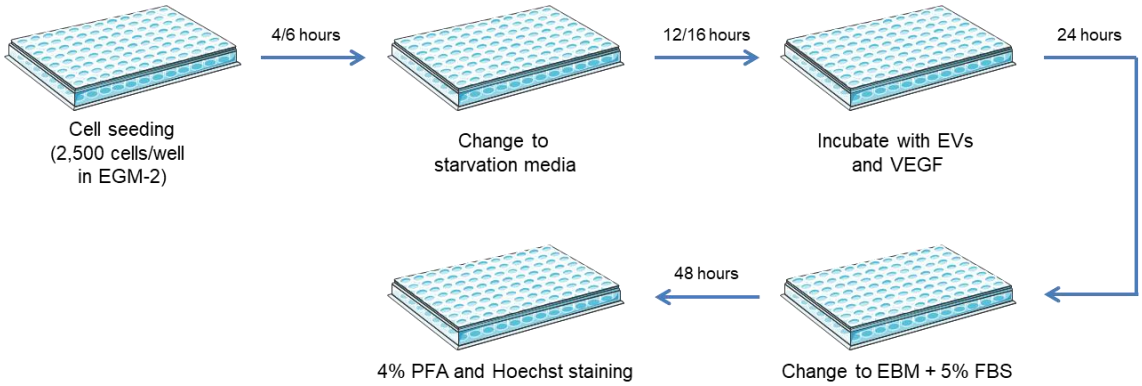

Figure 9 – Schematic representation of the proliferation assay.

3.7.2. Survival assay

In this assay, HUVECs were subjected to ischemic conditions (0.1% of O_2, 5% of CO_2 and FBS-EV depleted EBM supplemented with 1% (v/v) of FBS) in a hypoxic chamber and their survival was evaluated.

For that, 5.000 HUVECs per well were plated, left to adhere, starved, incubated 24 hours with FBS-EV depleted EGM-2 medium containing EVs or VEGF, as previously described in the proliferation assay. After the 24 hours of incubation, nuclear staining was performed to obtain the cell number before the ischemic condition (T0). Then, the media was discarded and FBS-EV depleted EBM supplemented with 1% (v/v) FBS was added to the cells, the plate was covered with sealing membrane (BreathEasy®; Sigma-Aldrich, Missouri, U.S.A., catalogue number: Z380059) and incubated for 48 hours in the hypoxic chamber (0.1% of O_2 and 5% of CO_2). After the 48 hours of incubation, the medium was discarded, cells were washed with PBS, fixed with PFA, the cell nuclei was stained and nuclear counts were obtained using a high-content image microscope (see details below in chapter 3.8 and 3.9), obtaining the cell number at T48 (figure 10). To get the percentage of cell survival per well, the next formula was used:

$$\%\ of\ survival = \frac{Cell\ number\ at\ T48}{Cell\ number\ at\ T0} \times 100$$

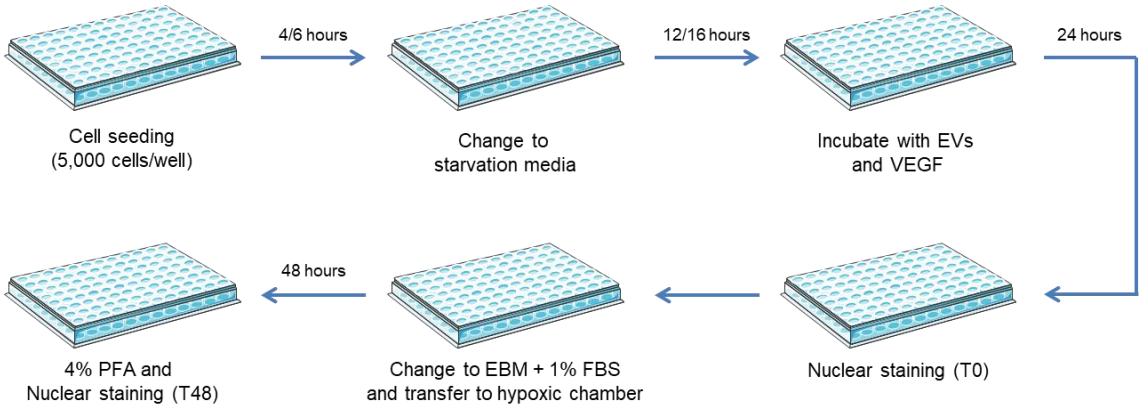

Figure 10 – Schematic representation of the survival assay.

3.7.3. Migration assay

For the migration assay, 10.000 HUVECs per well were plated, left to adhere, starved, incubated 24 hours with FBS-EV depleted EGM-2 medium containing EVs or VEGF, as previously described in the proliferation assay. After the 24 hours of incubation, a scratch was performed directly on the 96-well plate using a 200 µL pipette tip. In order to remove unattached cells of the cell layer, the media was discarded and one washing step with EBM was performed. Then, FBS-EV depleted EBM supplemented with 5% (v/v) FBS was added to the cells and one bright-field image per well at 4x magnification was acquired (see details below in chapter 3.8 and 3.9) every two hours between 0 hours and 12 hours, counting from the scratch moment (figure 11). Wound area recovery was measured using the open-source image processing software Fiji/ImageJ.

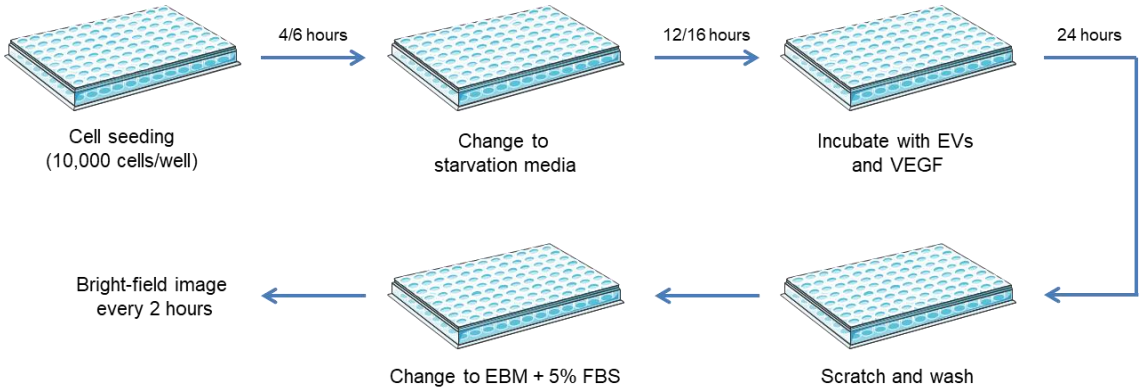

Figure 11 – Schematic representation of the migration assay.

3.8. Cell fixation and nuclear staining

Cells grown in 96-well plates were washed once with 100 µL of PBS and then fixed with 50 µL of 4% (v/v) of PFA for at least 10 minutes at room temperature. After fixation, PFA was discarded and the cells were washed with 100 µL of PBS and incubated in dark environment with 40 µL of 10 ng/mL of Hoechst for at least 10 minutes at room temperature. Then, Hoechst solution was discarded and the cells were washed 3 times with 100 µL of PBS and 100 µL of PBS was added in each well for image acquisition.

3.9. Image acquisition and analysis

The InCell Analyzer 2200 automated high-content imager (GE Healthcare) was used to acquire the images. For the migration assay, only one bright-field image per well was acquired using 4x magnification. Regarding the nuclear staining, 8 randomly selected bright-field and fluorescent images (DAPI channel) were acquired per well using 20x magnification. Cell counting was performed using the InCell Investigator software (GE Healthcare).

3.10. Statistical analysis

All the results presented in this work are shown as an average of the number of samples for each condition and standard deviation (SD). For each condition, at least 5 replicates were performed. Statistical testing was performed using GraphPad Prism® 6.0 software. The statistical tests used in this work consisted in Wilcoxon test, two-tailed Pearson correlation coefficient, one-way and two-way ANOVA with Tukey's multiple comparisons test correction. A probability value <0.05 was considered statistically significant.

3.11. Ethical Issues

Samples were obtained from patients from the cardiology department of the Centro Hospitalar e Universitário de Coimbra (CHUC). For all the participants in this study an informed consent was given. This study was

approved by the Ethics Commission of the Faculty of Medicine of the University of Coimbra with the reference numbers 092-CE-2017 and 041-CE-2018.

4. Results

4.1. Optimization of urine EVs isolation

As previously mentioned, urine is a rich source of EVs but the high levels of THP decrease the yield and purity of EVs isolated from this biofluid. To overcome this problem, we adapted a protocol described by Puhka *et al.* in which urine was diluted with tris-EDTA (T-EDTA) to disrupt THP aggregates.

For that, urine from 6 donors (3 males and 3 females) was used undiluted, diluted 4 times in PBS or in T-EDTA and vortexed thoroughly. Then, EVs were isolated using differential ultracentrifugation and characterized with classical techniques, such as NTA, zeta potential and microBCA.

To assess the yield we measured the total number of particles using NTA. Our results showed that, compared with undiluted samples, the particle number increased in 5 of the 6 samples upon dilution with both PBS and T-EDTA, although without reaching statistical significance (figure 12A). Interestingly, we observed a pronounced reduction in total protein upon dilution of urine samples with PBS or T-EDTA suggesting that diluted urine samples have less protein contaminants (figure 12B). Based on these results, we proposed that the number of particles per µg of protein would provide a measure of sample purity (figure 12C). In fact, using this parameter, we showed that, overall, there was a statistically significant increase in purity when urine samples were diluted with either PBS or T-EDTA. Also, EVs from urine diluted with T-EDTA had a purity higher than urine diluted with PBS dilution, with a statistical significant difference ($p\text{-value}<0.05$). Based on these results, and despite the donor variability observed in the procedure, we suggest that urine samples should be diluted with T-EDTA in order to increase both the yield as well as the purity of urine EVs (figure 12A, B and C).

Given the fact the EVs membranes comprise mostly lipids, one would expect a negative zeta potential for these particles. As expected, our results showed that urine EVs have a negative zeta potential ranging between -15.7 and -25.4 mV for undiluted samples (figure 12D). Importantly, upon dilution with either PBS or T-EDTA, we did not observe any significant changes in zeta

potential compared with undiluted samples showing that the dilution did not affect surface charge (PBS: -13.6 to -25.9 mV; T-EDTA: -18.3 to -26.7 mV).

In addition to the above-mentioned parameters we analysed the size distribution of urine EVs using NTA. A representative NTA profile for the size distribution of EVs from urine sample can be seen in figure 12E. Remarkably, within the same donor, the EVs mean size tends to increase upon dilution with either PBS or T-EDTA although only the later reached a statistically significant difference (p-value<0.05; figure 12F). Both mean size and mode of EVs from undiluted urine (mean size: 129.4 nm; mode: 109.5) were lower than urine diluted in PBS (mean size: 158.6 nm; mode: 123.1) or T-EDTA (mean size: 169.7 nm; mode: 126.1). Based on the above-mentioned, subsequent analyses were performed solely on undiluted or T-EDTA diluted samples.

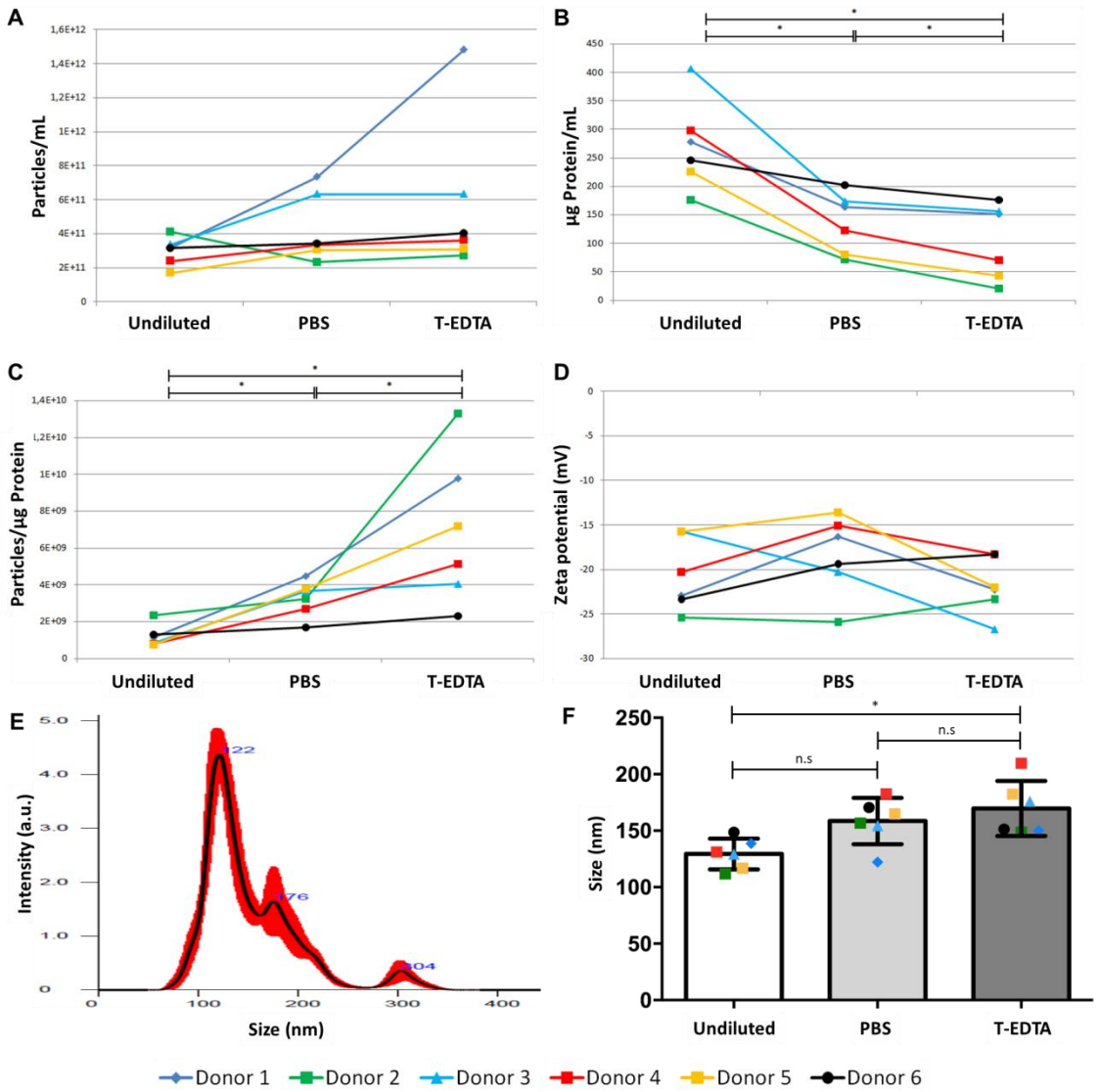

Figure 12 – T-EDTA dilution increases the yield and purity of urine EVs. **A)** Particles per mL were measured using NTA; **B)** Total amount of µg of protein per mL was obtained using microBCA^{TM} kit; **C)** Particles per µg of protein was used to assess EV purity; **D)** Surface charge (zeta-potential) of EVs; **E)** NTA profile of EVs from T-EDTA diluted urine from donor 6; **F)** Size diameter comparison between the conditions, obtained by NTA. Six samples were used for the urine EVs isolation optimization. Bars represent mean ± SD. An asterisk (*) denotes statistical significant difference (Two-tailed Wilcoxon matched-pairs test; $p< 0.05$).

4.2. Characterization of urine EVs by flow cytometry

To confirm the presence of EVs obtained from undiluted or T-EDTA diluted samples, classical EV markers were analysed by FC using aldehyde/sulfate latex beads. To optimize the protocol, we used an antibody against CD9 and, while maintaining the number of beads constant (5 uL), we increased the number of particles (5.0×10^9, 1.0×10^{10}, 2.5×10^{10} and 5.0×10^{10} particles).

Our results demonstrated that for urine EVs from undiluted urine, even with low amounts of EVs (5.0×10^9 particles) 97.3% of the events were $CD9^+$ (figure 13 – left column). Unexpectedly, we did not see an increase of $CD9^+$ EVs upon increasing the number of particles since, regardless of the particle concentration, $CD9^+$ events were always higher than 80%, suggesting the presence of contaminants capable of reacting with the aldehyde groups present in the beads (in these preparations the concentration of protein was 3 times higher than in the same number of particles of EVs from T-EDTA diluted urine).

In contrast, when using EVs from urine diluted with T-EDTA, we were able to observe an increase of $CD9^+$ events when increasing the particle concentration (figure 13 – right column). For example, when we used 5.0×10^9 particles, 26% of the events were $CD9^+$ and, doubling the amount of particles led to an almost two-fold increase in the percentage of $CD9^+$ events (49.2% of $CD9^+$ events). Interestingly, using an input of 2.5×10^{10} particles, the percentage of $CD9^+$ events was 66.2% and by doubling the number of particles a similar percentage was obtained (64.3% of $CD9^+$ events) suggesting that a plateau of particles per bead was reached.

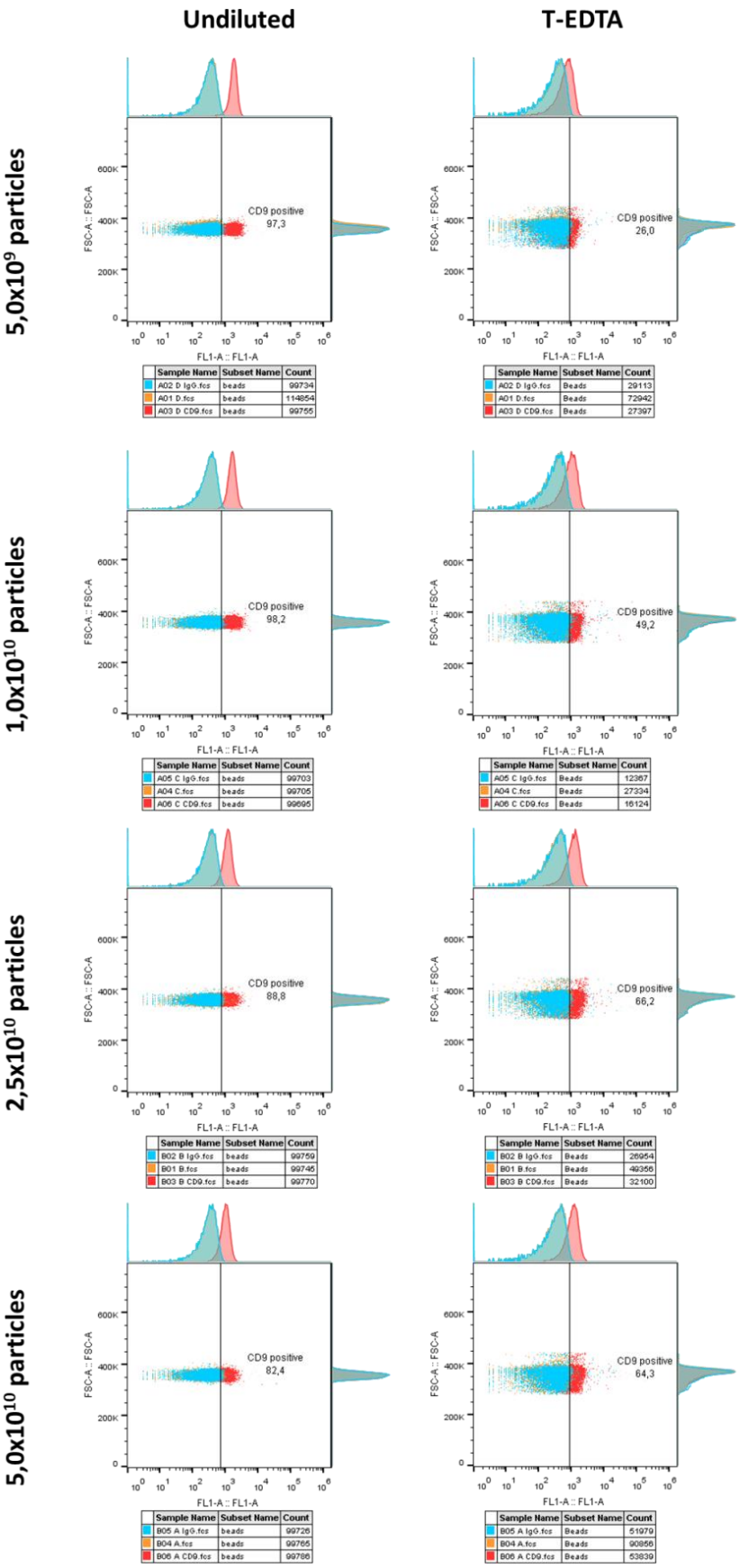

Figure 13 – Optimization of flow cytometry conditions using CD9 antibody. Different number of particles isolated from undiluted (left column) or T-EDTA diluted (right

column) urine were incubated with 5 µL of latex beads. The high percentage of $CD9^+$ events in all the conditions using EVs from undiluted urine suggests the presence of contaminants in the sample. On the contrary, using EVs from T-EDTA diluted urine, we showed an increase in the percentage of $CD9^+$ events with increasing concentrations of particles although a plateau was reached for 2.5 x 10^{10} particles.

Based on these results, we proceeded to analyse the percentage of $CD9^+$, $CD63^+$ or $CD9^+CD63^+$ EVs from urine samples obtained from T-EDTA diluted urine using 2.5 x 10^{10} particles per sample (Table 1). Our results showed that both markers were expressed in EVs isolated from T-EDTA diluted urine but there was a high inter-donor variation (for example, the percentage of $CD9^+CD63^+$ EVs varied between10.5% for donor 6 and 99.1% for donor 1 and similar variations could be observed for the single staining.

Table 1 – Expression of $CD9^+$, $CD63^+$ or $CD9^+CD63^+$ of EVs from T-EDTA diluted urine.

Donor	CD9	CD63	CD9 + CD63
Donor 1	98,3%	97,7%	99,1%
Donor 2	94,3%	96,8%	96,0%
Donor 3	43,0%	24,6%	12,4%
Donor 4	72,0%	53,8%	53,0%
Donor 5	57,0%	96,8%	61,3%
Donor 6	28,8%	19,1%	10,5%

4.3. Characterization of EVs from urine by TEM

Results obtained by FC suggest that we were able to isolated EVs from urine. However, TEM analysis was performed in order to show the presence of EVs and to analyse the presence of potential contaminants in undiluted samples, as suggested by the FC results.

EVs isolated from undiluted and T-EDTA diluted urine from one donor (donor 6) were submitted to TEM analysis and, as expected, we could observe the presence of filamentous contaminants in the undiluted condition (red arrows, figure 14) suggestive of the presence of THP aggregates (figure 14A,

left). Interestingly, upon dilution of the urine with T-EDTA, the amount of filamentous contaminants was significantly decreased corroborating our previous results. Furthermore, in both preparations, we could observe the presence of round-shape particles, a typical morphology of EVs (blue arrows, figure 14). Interestingly, the number of EVs seemed to be higher in the T-EDTA diluted urine suggesting that, as expected, the dilution of urine with T-EDTA led to a reduction in the number of THP aggregates with a concomitant increase in the number of "free" EVs (figure 14A, right). These results were consistently observed in all the images acquired in each condition.

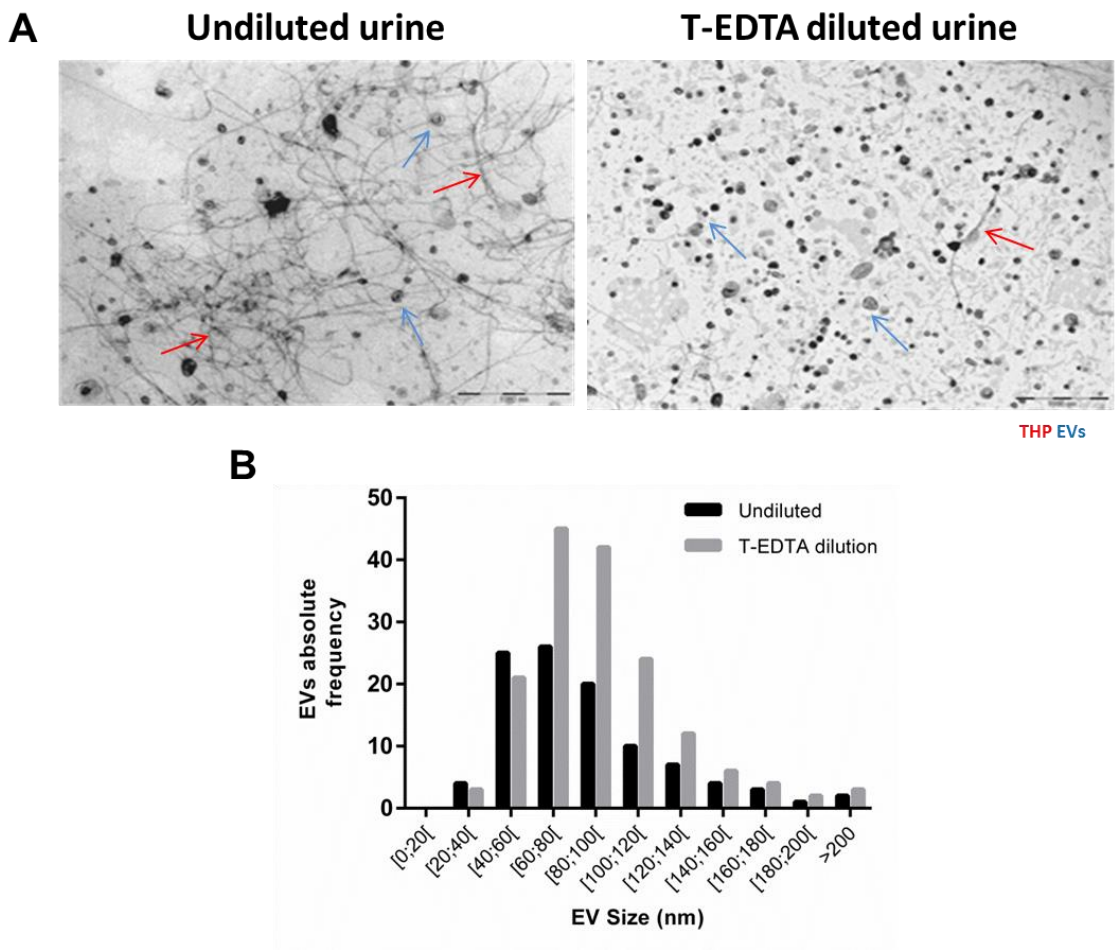

Figure 14 – TEM analysis of urine EVs from donor 6. **A)** Images of EVs obtained from undiluted (left) and T-EDTA diluted (right) urine. The image on the left shows EVs and the presence of contaminant protein. Upon dilution with T-EDTA, there was an increase on the number of EVs per field and a reduction of contaminant protein. **B)** EVs size distribution by TEM in both undiluted and T-EDTA diluted urine, showing an increase of EVs ranging from 60 to 140 nm in T-EDTA dilution condition. Red arrows indicate protein contaminants and blue arrows indicate EVs.

THP, Tamm-Horsfall protein; EVs, extracellular vesicles.

Then, we decided to evaluate EVs size by analysing the images with image processing software (ImageJ). For the undiluted sample, we measured a total of 832 EVs in 8 images whereas for T-EDTA diluted samples we measured 1794 EVs in 11 images. We normalized the number of EVs per image and distributed the size of the particles in different classes. Interestingly, we found that using T-EDTA there was enrichment on an EV subpopulation with a diameter between 60 and 140 nm (figure 14B). Also, we had an increase in mean size and mode between undiluted urine EVs (size: 87.3 ± 43.0 nm; mode: 51.0 nm) and T-EDTA diluted urine (size: 93.3 ± 37.6 nm; mode: 78.5 nm), which were in line with the increase observed previously using the NTA.

4.4. Cell media optimization for bioactivity assays

In order to identify the best medium to use in our bioactivity assays, we prepared media with different concentrations of FBS, ranging from 0% to 10% v/v), in the presence or absence of 50 ng/ml of VEGF and evaluated the proliferation rate of HUVECs. To that end, we used the PrestoBlue™ assay (a resazurin-based assay) to evaluate metabolic activity at 24 (figure 15A) and 48 hours (figure 15B) and, at 48h, in addition to the metabolic assay, we performed nuclear count using an image-based assay (figure 15D).

Our results showed that at 24 hours, in the presence of VEGF, HUVECs were metabolically more active than without VEGF (figure 15A). Interestingly, when HUVECs were cultured in EBM supplemented with FBS, we observed a plateau in metabolic activity at a concentration of 5% (v/v) FBS whereas in the presence of 50 ng/mL of VEGF this plateau was not observed (Figure 15A).

Strikingly, at 48 hours, we observed a decrease in metabolic activity when HUVECs were cultured in EBM supplemented with less than 5% (v/v) of FBS (figure 15B and C), suggesting that cell death occurred in these conditions even though, in the presence of 50 ng/mL of VEGF that effect was ameliorated. In contrast, when HUVECs were cultured in EBM supplemented with 5 or 10% (v/v) of FBS, an increase in metabolic activity between 24 and 48h was observed suggesting that, when basal medium alone is used, the medium must

be supplemented with at least 5% (v/v) FBS (Figure 15B and C). Furthermore, based on metabolic activity as well as on the nuclear count, we showed that, regardless of the presence of VEGF, HUVECs reached a plateau in the presence of 5% (v/v) FBS (figure 15D and E). In fact, Pearson correlation test showed a strong correlation between PrestoBlue™ and cell number at 48h ($r = 0.9487$; $R^2 = 0.9001$; 95% confidence interval [0.8420; 0.9840]; p-value<0.0001) (figure 15E).

Noteworthy, our results showed that when HUVECs were grown in EGM-2, the addition of 50 ng/mL of VEGF did not enhance proliferation suggesting that the composition of EGM-2, by itself, was sufficient to elicit a strong proliferative response.

Based on the results above we decided to proceed our studies with EBM supplemented with 5% (v/v) FBS since in this condition it was possible to maintain the cells alive and, upon addition of 50 ng/mL of VEGF, we could still observe a statistically significant increase in proliferation.

The statistical analysis concerning the experiments above can be seen in annex 8.1.

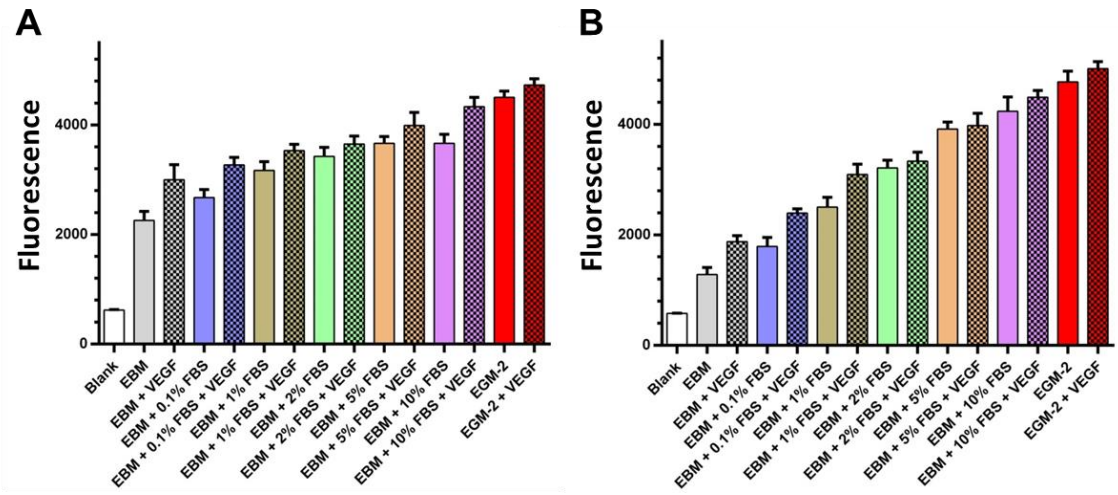

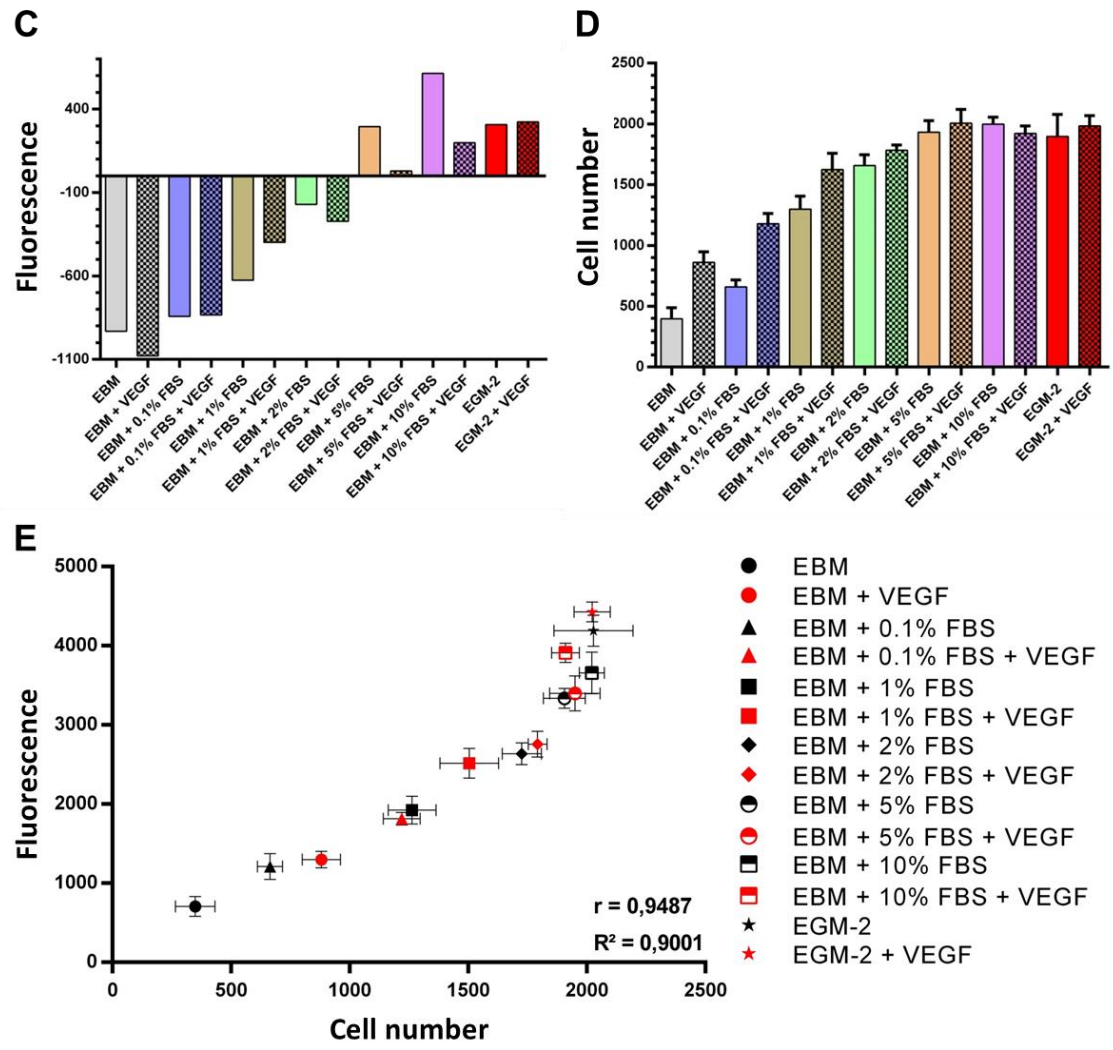

Figure 15 – Cell media optimization for bioactivity assays using a proliferation assay in HUVECs. Different concentrations of FBS in EBM were tested, ranging between 0% and 10% (v/v). EGM-2 was used as positive control. **A)** Metabolic activity measurement by PrestoBlue™ at 24 hours. **B)** Metabolic activity measurement by PrestoBlue™ at 48 hours. **C)** PrestoBlue™ delta results of 48 hours against 24 hours. **D)** Cell number quantified by nuclear staining and image-based analysis at 48 hours. **E)** Correlation between PrestoBlue™ and cell number results at 48 hours. Seven replicates were performed per condition (n = 7). Bars represent mean ± SD. Statistical analysis was performed using one-way ANOVA with Tukey's multiple comparisons test correction and two-tailed Pearson correlation coefficient. For the statistical analysis please see annex 8.1.

EBM, endothelial basal medium; FBS, fetal bovine serum; VEGF, vascular endothelial growth factor.

4.5. Bioactivity assays using EVs from urine of healthy donors

After establishing the best protocol for the isolation of EVs from urine as well as identified the best medium, we proceeded to test bioactivity of urine EVs in ECs. For that, HUVECS were incubated with 3 different concentrations of urine EVs (1.5 x 10^9, 3.0 x 10^9 and 4.5 x 10^9 part/mL) isolated from healthy donors and cell proliferation, survival and migration assays were performed.

Our results showed that urine EVs from healthy donors were capable of enhancing HUVECs proliferation although the concentration at which that effect was observed was donor-dependent (figure 16A). For example, for the donor H1, a statistically significant increase in cell proliferation was only observed at 4.5 x 10^9 part/mL (p-value<0.05), for donor H2, a statistically significant effect was observed in all the concentrations tested and for donor H3 a statistically significant effect was observed only at 1.5 x 10^9 part/mL (p-value<0.01). Interestingly, for donor H2 and H3, we observed a decrease in cell proliferation at the highest concentration of particles (4.5 x 10^9 particles/mL).

In the case of cell survival, urine EVs from healthy donors did not have effect on cell survival (figure 16B). Similarly, in the case of cell migration, urine EVs from healthy donors did not enhance cell migration at any of the time points analysed (figure 16C and D).

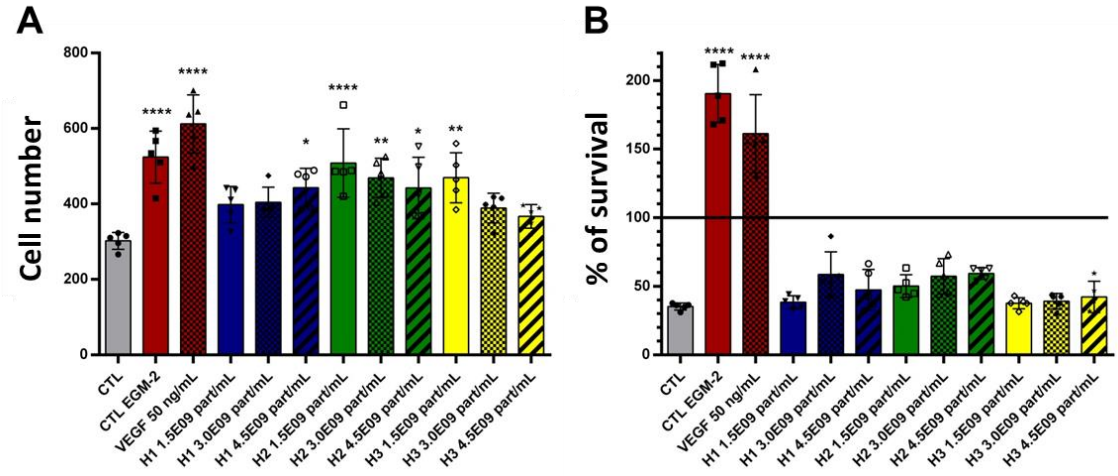

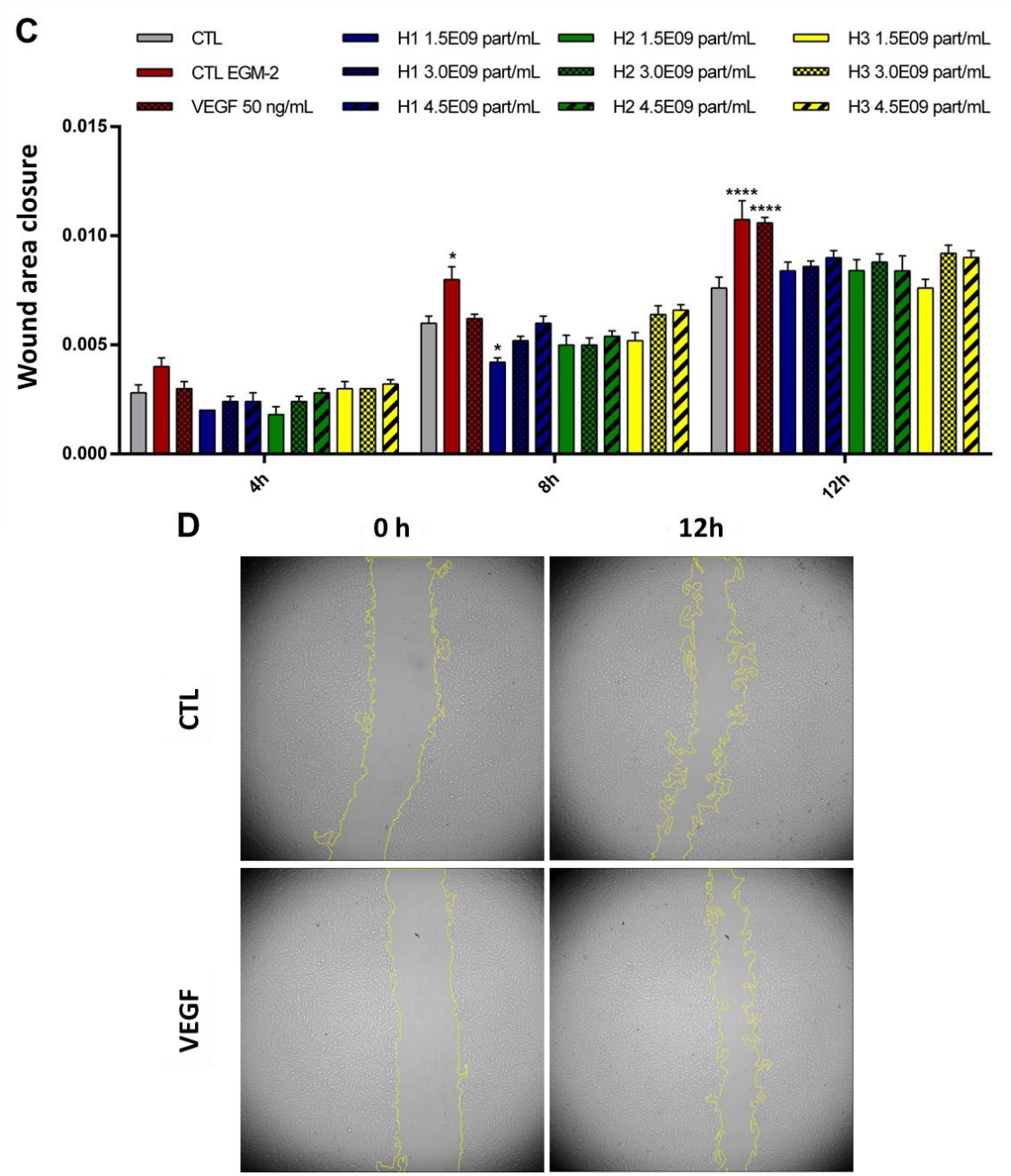

Figure 16 – Bioactivity assays results using urine EVs from three healthy donors. **A)** Results of cell proliferation assay. **B)** Results of cell survival assay. **C)** Results of cell migration assays. **D)** Example of the quantification of cell migration based on the area covered after 12 hours in control and VEGF conditions. Five replicates were performed per condition (n = 5). Bars represent mean ± SD. Statistical analysis of cell proliferation and survival assays was performed using one-way ANOVA and in cell migration assay was used two-way ANOVA, both with Tukey's multiple comparisons test correction. * $p<0.05$; ** $p<0.01$; *** $p<0.001$; **** $p<0.0001$

CTL, control; H, healthy donor; EGM-2, endothelial growth medium 2; VEGF, vascular endothelial growth factor.

Overall, our results showed that urine EVs isolated from healthy donors enhance, in a donor-dependent manner, EC proliferation but did not have an effect on EC survival and migration at the concentrations tested herein.

4.6. Bioactivity assays using EVs from urine of AMI patients

We hypothesize that after an AMI, given the proinflammatory and ischemic environment ensuing, the EV content could be different from normal healthy donors and thus elicit a different biological response.

To test this, we have repeated the bioactivity assays described above but this time using EV derived from urine of AMI patients. Furthermore, in order to understand if the content from urine EV derived from AMI patients changed during time, we isolated EVs at three different time points (<6h after admission, day 2 and day 3 after hospital admission) and, per time point, we used three different concentrations of EVs (1.5×10^9, 3.0×10^9 and 4.5×10^9 part/mL).

In the survival assay, and similarly to urine EVs from healthy donors, EVs from both AMI patient (figure 17C and D) did not enhanced the survival of HUVECS. In fact, 1.5×10^9 part/mL of EVs from day 2 (p-value<0.05) and 3.0×10^9 and 4.5×10^9 part/mL from day 3 (p-value<0.01 and <0.5, respectively) of AMI1 patient (figure 16C) had a negative effect on HUVECs survival.

Ours results showed that EVs from urine of both patients could enhance EC proliferation (figure 17A and B) and migration (figure 17E and F) although the extension of the response was different between patients. Using 1.5×10^9 part/mL of EVs isolated from day 1 of AMI1 patient did not enhanced EC proliferation (figure 17A). Nonetheless, a statistical significant increase was observed for all the remaining concentrations and days tested. In fact, the lowest concentration of EVs from day 3 had a similar effect on proliferation as 50 ng/mL VEGF (p-value<0.0001). On the contrary, for AMI2 patient (figure 16B) only when we used 4.5×10^9 part/mL of EVs from urine of day 2 and day 3, were able to enhance cell proliferation, with p-values of 0.05 and 0.01, respectively.

In the case of migration, all the concentrations of EVs from AMI1 for all the days tested led to an increase in cell migration reaching a statistical

significant difference at 8 hours (figure 17E). However, after 12 hours, for the concentration 3.0 x 10^9 part/mL at day 1 and day 3, the positive effect was lost. Interestingly, all the concentrations of EVs from the day 2 were statistical significant different from the control and only two concentrations from day 1 and day 3 were statistically significantly different. However, at least one of the EVs concentrations tested from each day had an effect on migration similar to the positive controls VEGF and EGM-2 ($p<0.0001$). Regarding the urine EVs from the AMI2 patient (figure 17F), at 12 hours, only the concentration 4.5 x 10^9 part/mL from day 1 had a statistically significant difference compared with the control (p-value<0.05). All the other concentrations tested from day 2 and day 3 increased HUVECs migration with statistical significance.

Interestingly, results from both cell proliferation and migration assays behaved similarly for urine EVs from both donors despite the fact that the effects seemed more pronounced for EV isolated from AMI1 patient (figure 17A and E and figure 17B and F).

Overall, our results suggest that EVs isolated from the urine of AMI patients have different bioactivity than EV isolated from healthy donors suggesting that their molecular signature (both intracellular as well as cell membrane receptors) may differ from EV isolated from healthy donors urine.

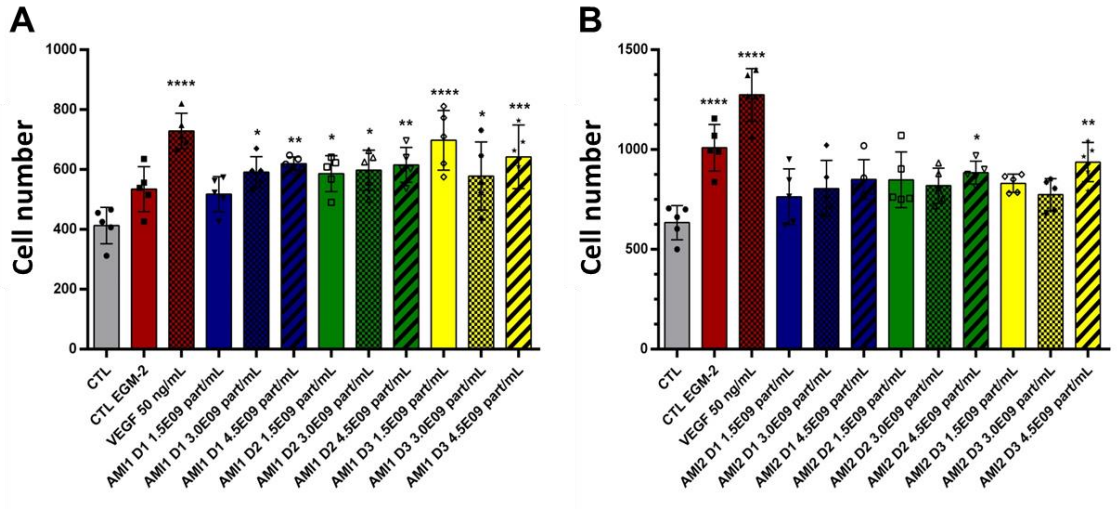

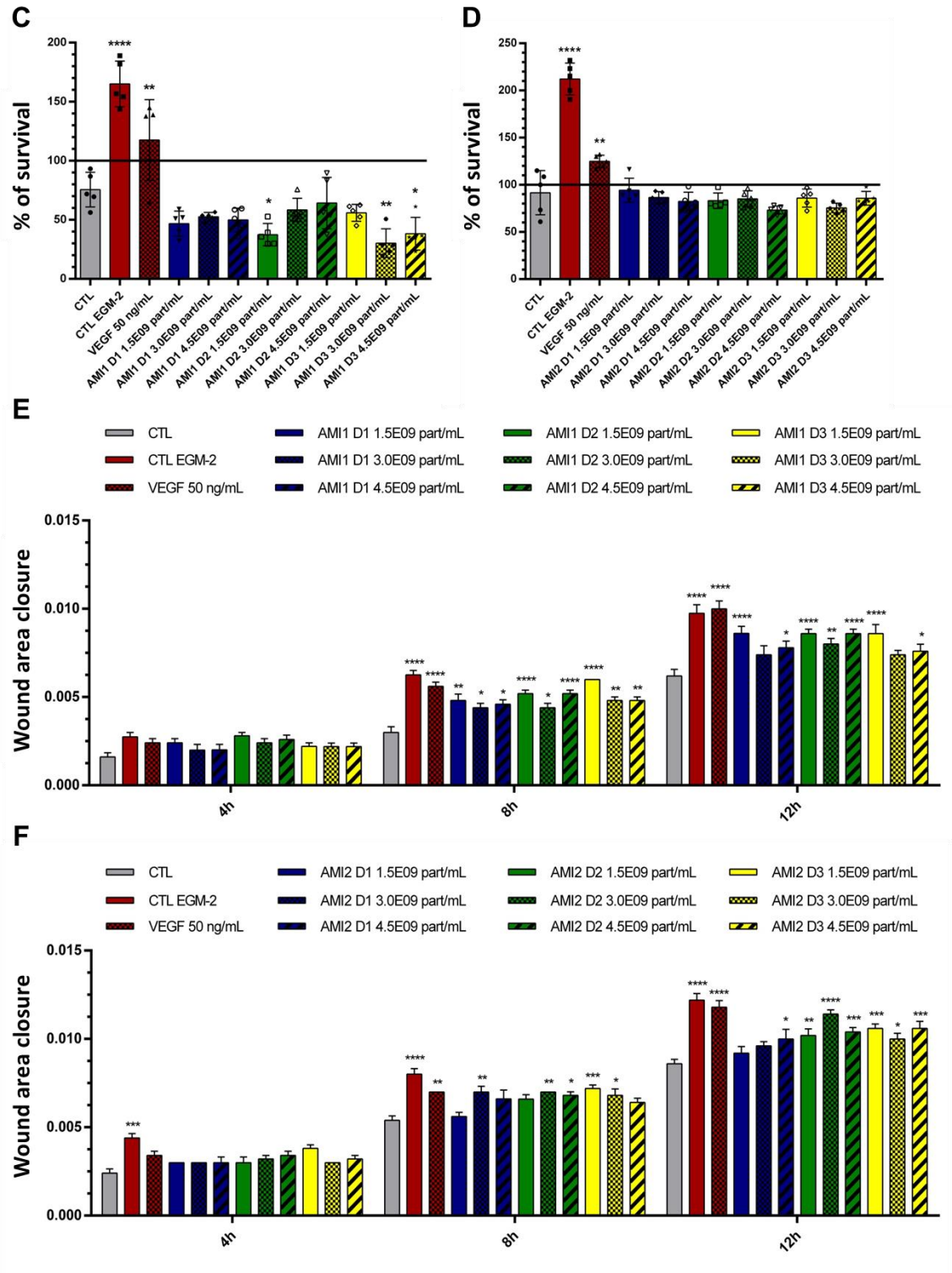

Figure 17 – Bioactivity assays results using urine EVs from two AMI patients. **A)** and **B)** Results of cell proliferation assay of the AMI patient 1 and 2, respectively. **C)** and **D)** Results of cell survival assay of the AMI patient 1 and 2, respectively. **E)** and **F)** Results of cell migration assays of the AMI patient 1 and 2, respectively. Five replicates were performed per condition (n = 5). Bars represent mean ± SD. Statistical analysis of cell proliferation and survival assays was performed using one-way ANOVA and in cell

migration assay was used two-way ANOVA, both with Tukey's multiple comparisons test correction. * $p<0.05$; ** $p<0.01$; *** $p<0.001$; **** $p<0.0001$

CTL, control; AMI, acute myocardial infarction patient; D, day; EGM-2, endothelial growth medium 2; VEGF, vascular endothelial growth factor.

5. Discussion

In the last decade, the number of publications referring to EVs has grown exponentially[110]. EVs have been studied in order to evaluate their function in cell biology as well as their potential as biomarkers and therapeutic agents[51,64,111].

EVs have been isolated from diverse biofluids, such as blood, urine, breast milk, amongst others[94–97]. In fact, urine is a great source of EVs since it can be collected non-invasively in large amounts and it is frequently used for biomarker identification[99]. However, urine contains THP, a contaminant protein that usually forms networks or gel-matrix aggregates that contaminate EV preparations and consequently reduce the EV yield, through their entrapment and precipitation at low speed centrifugations[99,104,107]. Puhka *et al.* reported that dilution of urine with Tris-HCl or Tris-HCl with EDTA (T-EDTA) disrupted THP aggregates preventing their precipitation during low speed centrifugations and ultimately increasing the number of EVs[99]. However, it was unclear if the effect was due to the dilution itself or due to the T-EDTA buffer.

Here, in addition to the dilution with T-EDTA buffer (20 mM of Tris-HCL and 20 mM of EDTA, pH 9.0) we decided to test the isolation of EVs using also undiluted or PBS-diluted urine. Using this strategy, we were able to show that the dilution with PBS or T-EDTA increased the number of EVs, as measured by NTA, in 5 of 6 healthy donors tested, being the yield higher in the conditions diluted with T-EDTA. Interestingly, the effects of the dilution were donor-dependent with one donor showing a decrease in the yield whereas the other five showed an increase, with a maximum increase of 465% compared to undiluted samples (figure 12A). These results are in line with the findings originally reported by Puhka *et al.* since they also showed an increase of EV number in 5 of their 6 samples, with an yield ranging from 1000% increase to a 48% of decrease upon dilution[99]. If we combine the results of both studies we can conclude that the dilution of urine with T-EDTA buffer increases the yield of EVs in 83.3% of the samples (n = 12).

In addition to increase the yield, Puhka *et al.* showed an increase in EV purity upon dilution[99]. Our results corroborated their findings since upon dilution

with PBS or T-EDTA, we showed a statistically significant decrease in the total amount of protein (figure 12B). Based on this observation, we decided to use the ratio particles per µg of protein as a measure of purity for EV preparations (figure 12C). In fact, Webber and Clayton used this measure in 2013 to assess EV purity from different sources, including urine[112]. Based on their results, they devised a purity scale in which a ratio of particles per µg of protein under 1.5 x 10^9 is an impure sample, between 1.5 x 10^9 and 2 x 10^{10} particles per µg of protein was a low purity sample and above 3 x 10^{10} particles per µg of protein the samples were considered highly pure[112]. Interestingly, their urine EV isolation protocol with a washing step with PBS was equivalent to our undiluted condition protocol. Based on their scale, 4 of the 6 samples that we used to isolate EVs from undiluted urine were impure and 2 of them were in the lower limit of low purity preparation. However, the EVs isolated from urine diluted in PBS and T-EDTA ranged between 1.7 x 10^9 and 4.5 x 10^9 particles per µg of protein and between 2.3 x 10^9 and 1.3 x 10^{10} particles per µg of protein, respectively, which corresponds to low to intermediate purity. Overall, the results obtained suggest that the urine dilution, either with PBS or T-EDTA, increases the purity of EVs being the dilution with T-EDTA more effective than with the dilution with PBS.

In a recent study published by Liu *et al.*, the authors reported a simple protocol to reduce THP in urine EV preparations[94]. Using electrophoresis, the authors showed that addition of 1 mM of $ZnSO_4$ to urine will eliminate the presence of THP. Moreover, the addition of $ZnSO_4$ before storage at -20 ºC or -80 ºC reduces THP contamination of urine EVs. They propose that $ZnSO_4$ may interfere with THP oligomerization in two ways: either leading to the formation of smaller aggregates which remain in the supernatant or, conversely, by forming bigger aggregates that are eliminated at low speed centrifugations. Nevertheless, despite a reduction in THP, they were not able to observe an increase in the number of urine EVs, compared with untreated samples, upon addition of $ZnSO_4$. Comparing this protocol with the one herein described we were able to obtain 10^{11} to 10^{12} part/mL using our protocol whereas using $ZnSO_4$ the reported yield was around 10^{10} part/mL. It would be interesting to

test whether combining T-EDTA dilution with the addition of $ZnSO_4$ would lead to higher yield and purity of urine EVs.

Our EV preparations showed a negative zeta potential (figure 12D), which is a feature of biological vesicles and indicative of the presence of phospholipids. Additionally, our EVs had sizes that were within the range reported for exosomes, between 30 and 200 nm of diameter[86]. Still, these properties are not exclusive of exosomes and may be found in other biological vesicles, such as microvesicles. The biogenesis and secretory pathway of exosomes is what truly distinguishes them from other vesicular entities. Thus, it is still challenging to unequivocally demonstrate that vesicles, especially those from a biofluid, are exosomes per se[41]. In contrast with the results reported by Puhka *et al.* in which the dilution with any buffer did not changed the EV size[99], and based on NTA measurements, we obtained vesicles with different sizes depending on the condition used for the isolation (figure 12F). In general, within the same donor, the mean size of EVs increased upon dilution with PBS or T-EDTA. This observation was corroborated by TEM where we observed an enrichment of a specific EV subpopulation from 60 to 140 nm of diameter upon dilution with T-EDTA (figure 14B). We hypothesize that, upon dilution of urine with T-EDTA, THP aggregates were disrupted and a specific size-based subpopulation of EVs entrapped on that protein network was released, avoiding their elimination on the low speed centrifugations (figure 18).

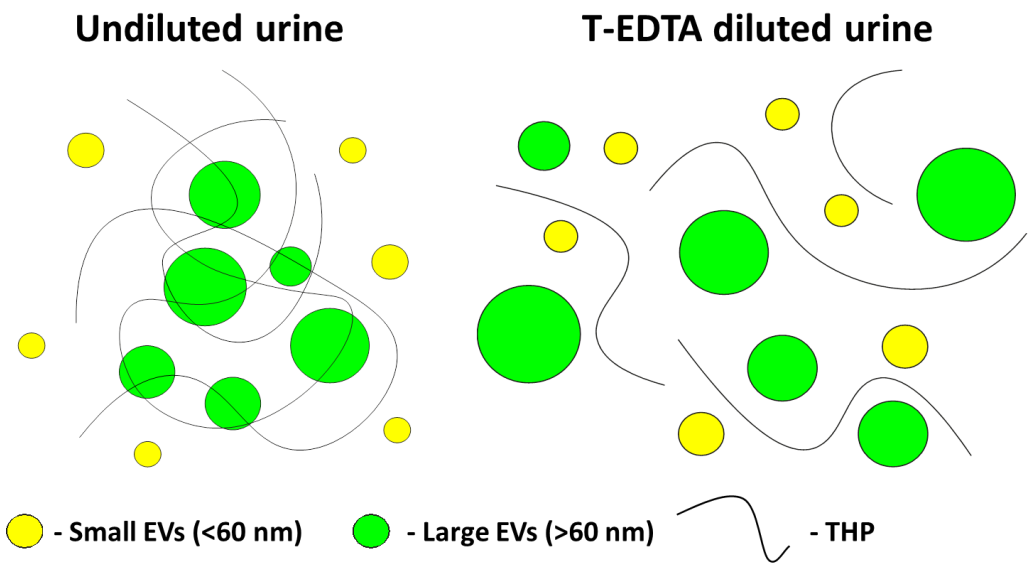

Figure 18 – Schematic representation of the effect of T-EDTA dilution on THP found in urine. Without the dilution of the urine (left image), THP aggregates entrapped a

specific subpopulation of EVs larger than 60 nm of diameter. Those EVs were eliminated in steps of low speed centrifugation, since large proteins aggregates were pelleted and, consequently, EVs were removed. T-EDTA dilution of the urine (right image) prevented the aggregation of THP, with the concomitant release of EVs. In that case, lower quantities of EVs were eliminated in the low speed centrifugations steps since there was a reduction in protein aggregates with EVs entrapped.

EVs, extracellular vesicles; nm, nanometer; T-EDTA, Tris-EDTA buffer; THP, Tamm-Horsfall protein.

In our TEM images we were also able to confirm the presence of round-shaped structures, as previously reported by Pisitkun *et al.* and Puhka *et al.*, suggestive of EVs and their morphology was not altered by the dilution with T-EDTA (figure 14A)[99,113]. Moreover, we could observe the presence of filamentous structures and aggregates in the TEM images, which are consistent with THP structures previously reported[99,114]. Interestingly, and compared with undiluted sample, we observed that the dilution with T-EDTA led to a reduction of these filamentous structures which is in line with our results of total protein quantification and respective purity (particles/µg of protein), supporting the notion that T-EDTA dilution yields a more pure fraction of urine EVs.

To characterize and confirm the presence of EVs in our preparations, we decided to analyze the presence of classical EV markers (CD9 and CD63) by FC. Surprisingly, the smallest concentration of EVs from undiluted urine had 97% of $CD9^+$ events and this percentage was maintained high regardless of the number of particles used. Interestingly, we observed that a high percentage of $CD9^+$ events were outside the region demarked by the bead size (3.8 µm) suggestive of the presence of protein aggregates containing entrapped EVs (result not shown). In contrast, when we used EVs from T-EDTA diluted urine, we could observe an increase in the percentage of $CD9^+$ events upon increasing the number of particles incubated with the beads until a plateau was reached at 2.5×10^{10} particles. For that reason, we used 2.5×10^{10} EVs from the T-EDTA diluted urine in order to measure the expression of both markers.

Using the above-described settings we were able to show that urine EVs express both CD9 and CD63 although in a donor-dependent manner, similarly to previous reports using WB to quantify their expression[99,113]. Curiously, Liu *et al.* reported that EVs isolated from urine using $ZnSO_4$ had a

similar expression of CD9[94]. Based on these results we conclude that our urine EVs express classical markers of EVs although the expression is dependent on the donor. Future work should focus on the analysis of these markers at a single EV level using adapted FC protocols[115–117]. Forward and side scatters of the cytometry analysis do not have the resolution to analyze single EVs since they are typically in the range of 100 nm or smaller, and have a poor refractive index. However, using fluorescent beads to calibrate the cytometer, it would be possible to subsequently use fluorescently labeled EVs and thus analyze the expression of markers on single EVs.

In the therapeutic field, EVs have gained much attention since reports showing that the beneficial effects of cell transplantation were not only due to the engraftment of cells but also to the paracrine factors released by the cells, in which EVs are included[118]. Furthermore, it is now recognized that EV content is usually altered in disease. In fact, Deddens *et al.* showed that after I/R injury in a porcine animal model, EVs from the heart were released to the blood and that heart-specific miRNAs (miR-1, miR-133b, miR-208b and miR-499) were increased in those EVs[27]. Interestingly, Cheng *et al.* showed that EVs collected from AMI rat urine had increased levels of miR-1[108]. Having this in mind, we hypothesized that the bioactivity of EVs from healthy donors and AMI patients could be different. For that reason, we decided to perform bioactivity assays in HUVECs using our EVs from the urine of healthy donors and AMI patients.

To test the therapeutic potential of urine EVs we decided to use ECs as the *in vitro* model. It is known that, after an ischemic event, circulating EPCs were increased and tend to engraft into the ischemic lesion, contributing to the formation of new blood vessels within the injury site[9,10,119,120]. In fact, angiogenesis mediated by the administration of ECs has been explored for the treatment of ischemic disease given their potential to repair the microvasculature of the affected area and ultimately decreasing the mortality associated with ischemic events[121–124].

Before we proceeded with the bioactivity assays we had to optimize the culture conditions for ECs, in particular the composition of the medium. EGM-2, the classical medium used for EC expansion, contains a myriad of growth factors such as Insulin-like Growth Factor (Long R3 IGF), Epidermal Growth

Factor (EGF), Basic Fibroblast Growth Factor (bFGF) and VEGF. Using such an enriched medium could potentially mask the effects of added EVs and this masking effect was indeed observed after adding extra VEGF to the EGM-2. Upon addition of 50 ng/mL of VEGF to EGM-2 we could not observe an increase on the proliferation of ECs suggesting that the original composition was sufficient to elicit a strong proliferative response. Therefore, we optimized the culture conditions in order to maintain EC viability and their proliferative capacity using solely EBM and different concentrations of FBS and ultimately we decided to proceed with EBM supplemented with 5% (v/v) of FBS (figure 15). When EVs were incubated with HUVECs, the medium was always FBS-EVs depleted in order to discard the potential interference of bovine EVs[41,86]. Using urine EVs from healthy donors we were able to see that these EVs do not have any effect on HUVEC survival and migration assays, but an increase of proliferation occurs (figure 16).

Interestingly, when we used urine EVs isolated from AMI patients we observed differences in their bioactivity compared with EVs from healthy donors, suggesting that the content of urine EVs from healthy and AMI patients was different. Urine EVs isolated from AMI1 patient <6h after admission to the emergency room (ER) already enhanced the proliferation and migration of HUVECs while EVs from AMI2 patient did not have any effect at the same time point (figure 17) despite the fact that the collection moment was similar since their admission to the ER. Interestingly, when we consider the onset of chest pain, a difference of 5 hours was observed between both patients which could account for the differences observed (table 2). Cheng *et al.* have shown kidney clearance of the free miR-1 (heart specific miRNA) in rats after AMI[108] and interestingly, they showed that miR-1 was enriched only at 12 hours and peaked at 24 hours after the AMI, decreasing afterwards. If urine EVs have a similar filtration pattern, this could explain the absence of effects of the EVs from the first urine collection of the AMI2 patient (<12 hours after the onset of symptoms).

Table 2 – AMI patient donor data

						Hours since chest pain		
Patient	**Gender**	**Age**	**Hospital admission day time**	**Day time that chest pain started**	**hs-cTnI (ng/L)**	**Urine collection <6 hours**	**Urine collection day 2**	**Urine collection day 3**
AMI 1	Male	58	22h26	10h30	62706,4	13h30	20h30	51h30
AMI 2	Male	67	13h56	10h00	2503,6	8h30	21h	45h

The hs-cTnI measurements can be an indirect measure of AMI extension. AMI1 and AMI2 hs-cTnI levels differ dramatically suggesting that AMI1 patient had a much bigger AMI than AMI2 (normal value for men is under 34 ng/mL). Since EV content might be dependent of infarction size this could justify why EVs from AMI1 patient have higher bioactivity than EVs from AMI2 patient.

EVs have been previously used for the treatment of chronic ischemia. Potz *et al.* have used MSC-derived EVs in swine model of chronic ischemia and showed that these EVs improved the myocardial function and also the capillary density in ischemic tissue[125]. Although we did not test the potential of our EVs on angiogenesis, proliferation and migration assays can work as makeshift surrogate for angiogenesis suggesting that the AMI patient EVs might have effect on angiogenesis[126].

To the best of our knowledge, we were the first to use urine EVs in bioactivity assays using ECs. Although these preliminary results seem promising we cannot exclude that other non-EV related factors can contributed to the observed outcome. First, the pellet of EVs isolated from urine of the first day in each AMI patient was thick. Our hypothesis is that the contrast agent (iodine solution, used for diagnostics/therapeutics purposes) is pelleted with the EVs in the last ultracentrifugation step. However, the urine EVs isolated from the first day of the AMI2 patient did not have any effect despite the fact that iodine was also present. Second, the EVs can have bioactivity but they do not necessarily have to be derived from cardiac cells. The systemic inflammation ensuing after an AMI episode might induce the release of EVs with different content and also from different organs such as, for example, the kidney. In fact, the relationship between the heart and kidney is well known[127–129]. After a heart

insult, acute renal injury can occur due to an acute hypoperfusion and concomitant reduction in the amount of oxygen delivery to that organ[127]. In that case, EVs with different content might be produced by an injured kidney and released to the urine, resulting from an indirect damage from the ischemic heart condition.

The use of EVs in regenerative medicine is becoming attractive since these natural vesicles are expected to be less toxic and more accepted by immunologic system than synthetic nanoparticles. However, Liu *et al.* have proved that EVs have the ability to present major histocompatibility complex (MHC) molecules to dendritic cells and as a consequence, alloreactive T cells were activated by the EVs-activated dendritic cells[130]. For that reason, autologous EVs could be a way to reduce the effect of the immunologic system and urine could be used as a potential source of EVs with many advantages for harvesting as well as for therapeutic purposes.

6. Conclusion and further perspectives

The field of EVs has grown in the last decades, arousing interest in both academia and corporate fields. The discovery of the presence of miRNAs and mRNA within EVs has linked these vesicles with pathological conditions of the cells. In fact, many studies have been performed using EVs as diagnostic/prognostic or therapeutic tools.

In this work we have stablished an optimized protocol for isolation of urine EVs. We were able to confirm that the dilution of urine and the effect of T-EDTA work synergistically to increase EVs yield and purity. The EVs isolated from urine were thoroughly characterized by size, morphology, purity, zeta potential and the expression of classical EV markers by FC.

Importantly, we showed that urine EVs can enhance the proliferation and migration of ECs although the effect was more pronounced when we used EVs isolated from urine of AMI patients. These results suggest that urine EVs from AMI patients can significantly help in the recovery after an ischemic heart condition. However, more studies are needed to fully understand our results.

Further studies need to be performed to unravel the mechanism behind the EVs effect. Several heart specific miRNAs (miR-1; miR-208a; miR-208b; miR-499) are enriched in the plasma after AMI. We should analyze the expression of these miRNAs in urine EVs from the AMI patients to understand if the EVs isolated from the urine are coming from the heart or result from an indirect effect triggered by the ischemic event. Furthermore, the number of AMI patients should be increased to add robustness to our results. Lastly, we should test these EVs in different type of cells and test the angiogenic potential on ECs.

7. References

1. Thygesen K, Alpert JS, Jaffe AS, Simoons ML, Chaitman BR, White HD. Third Universal Definition of Myocardial Infarction. *Glob Heart*. 2012;7(4):275-295. doi:10.1016/j.gheart.2012.08.001.

2. White H, Thygesen K, Alpert JS, Jaffe A. Universal MI definition update for cardiovascular disease. *Curr Cardiol Rep*. 2014;16(6):492. doi:10.1007/s11886-014-0492-5.

3. Uemura R, Xu M, Ahmad N, Ashraf M. Bone marrow stem cells prevent left ventricular remodeling of ischemic heart through paracrine signaling. *Circ Res*. 2006;98(11):1414-21. doi:10.1161/01.RES.0000225952.61196.39.

4. Pfeffer MA, Braunwald E. Ventricular remodeling after myocardial infarction. Experimental observations and clinical implications. *Circulation*. 1990;81(4):1161-1172. doi:10.1161/01.CIR.81.4.1161.

5. Coulombe KLK, Bajpai VK, Andreadis ST, Murry CE. Heart Regeneration with Engineered Myocardial Tissue. *Annu Rev Biomed Eng*. 2014;16(1):1-28. doi:10.1146/annurev-bioeng-071812-152344.

6. Pinto AR, Ilinykh A, Ivey MJ, et al. Revisiting Cardiac Cellular CompositionNovelty and Significance. *Circ Res*. 2016;118(3):400-409. doi:10.1161/CIRCRESAHA.115.307778.

7. Hsieh PCH, Davis ME, Lisowski LK, Lee RT. Endothelial-cardiomyocyte interactions in cardiac development and repair. *Annu Rev Physiol*. 2006;68(1):51-66. doi:10.1146/annurev.physiol.68.040104.124629.

8. Brutsaert DL. Cardiac endothelial-myocardial signaling: its role in cardiac growth, contractile performance, and rhythmicity. *Physiol Rev*. 2003;83(1):59-115. doi:10.1152/physrev.00017.2002.

9. Takahashi T, Kalka C, Masuda H, et al. Ischemia- and cytokine-induced mobilization of bone marrow-derived endothelial progenitor cells for neovascularization. *Nat Med*. 1999;5(4):434-438. doi:10.1038/7434.

10. Asahara T, Masuda H, Takahashi T, et al. Bone marrow origin of endothelial progenitor cells responsible for postnatal vasculogenesis in physiological and pathological neovascularization. *Circ Res*. 1999;85(3):221-8. Available at: http://www.ncbi.nlm.nih.gov/pubmed/10436164.

11. Lino MM, Simões S, Vilaça A, Antunes H, Zonari A, Ferreira L. Modulation of

Angiogenic Activity by Light-Activatable miRNA-Loaded Nanocarriers. *ACS Nano*. 2018. doi:10.1021/acsnano.7b07538.

12. Fan X, Teng Y, Ye Z, Zhou Y, Tan W-S. Gap junction-mediated MiR-200b on osteogenesis and angiogenesis in coculture between MSCs and HUVECs. *J Cell Sci*. 2018;106(4):jcs.216135. doi:10.1242/jcs.216135.

13. Fish JE, Srivastava D. MicroRNAs: Opening a new vein in angiogenesis research. *Sci Signal*. 2009;2(52):2-4. doi:10.1126/scisignal.252pe1.

14. Wang S, Aurora AB, Johnson BA, et al. The Endothelial-Specific MicroRNA miR-126 Governs Vascular Integrity and Angiogenesis. *Dev Cell*. 2008;15(2):261-271. doi:10.1016/j.devcel.2008.07.002.

15. Cowburn AS, Macias D, Summers C, Chilvers ER, Johnson RS. Cardiovascular adaptation to hypoxia and the role of peripheral resistance. *Elife*. 2017;6:1-23. doi:10.7554/eLife.28755.

16. Xiao J, Ke Z-P, Shi Y, Zeng Q, Cao Z. The cardioprotective effect of thymoquinone on ischemia-reperfusion injury in isolated rat heart via regulation of apoptosis and autophagy. *J Cell Biochem*. 2018;(September 2017):1-7. doi:10.1002/jcb.26878.

17. Minamino T. Cardioprotection From Ischemia/Reperfusion Injury. *Circ J*. 2012;76(5):1074-1082. doi:10.1253/circj.CJ-12-0132.

18. Buja LM. Myocardial ischemia and reperfusion injury. *Cardiovasc Pathol*. 2005;14(4):170-5. doi:10.1016/j.carpath.2005.03.006.

19. Behfar A, Crespo-Diaz R, Terzic A, Gersh BJ. Cell therapy for cardiac repair—lessons from clinical trials. *Nat Rev Cardiol*. 2014;11(4):232-246. doi:10.1038/nrcardio.2014.9.

20. Moss AJ, Zareba W, Hall WJ, et al. Prophylactic Implantation of a Defibrillator in Patients with Myocardial Infarction and Reduced Ejection Fraction. *N Engl J Med*. 2002;346(12):877-883. doi:10.1056/NEJMoa013474.

21. Cortés M, Palfy JA, Lopez M, et al. Comparison of pharmacological treatment alone vs. treatment combined with implantable cardioverter defibrillator therapy in patients older than 75 years. *ESC Hear Fail*. 2018. doi:10.1002/ehf2.12310.

22. Jørgensen ME, Andersson C, Venkatesan S, Sanders RD. Beta-blockers in non-cardiac surgery: Did observational studies put us back on safe ground? *Br J Anaesth*. 2018;10:1-10. doi:10.1016/j.bja.2018.02.004.

23. Healey JS, Baranchuk A, Crystal E, et al. Prevention of atrial fibrillation with angiotensin-converting enzyme inhibitors and angiotensin receptor blockers: A meta-analysis. *J Am Coll Cardiol*. 2005;45(11):1832-1839. doi:10.1016/j.jacc.2004.11.070.

24. Hirai T, Yamaga R, Fujita A, Itoh T. Low body mass index is a risk factor for hyperkalaemia associated with angiotensin converting enzyme inhibitors and angiotensin II receptor blockers treatments. *J Clin Pharm Ther*. 2018;(May):1-7. doi:10.1111/jcpt.12720.

25. Mair J, Lindahl B, Hammarsten O, et al. How is cardiac troponin released from injured myocardium? *Eur Hear journal Acute Cardiovasc care*. 2017:2048872617748553. doi:10.1177/2048872617748553.

26. Sandoval Y, Thygesen K. Myocardial Infarction Type 2 and Myocardial Injury. *Clin Chem*. 2017;63(1):101-107. doi:10.1373/clinchem.2016.255521.

27. Deddens JC, Vrijsen KR, Colijn JM, et al. Circulating Extracellular Vesicles Contain miRNAs and are Released as Early Biomarkers for Cardiac Injury. *J Cardiovasc Transl Res*. 2016;9(4):291-301. doi:10.1007/s12265-016-9705-1.

28. Parmacek MS, Solaro RJ. Biology of the troponin complex in cardiac myocytes. *Prog Cardiovasc Dis*. 2004;47(3):159-176. doi:10.1016/j.pcad.2004.07.003.

29. Katrukha IA. Human cardiac troponin complex. Structure and functions. *Biochemistry (Mosc)*. 2013;78(13):1447-65. doi:10.1134/S0006297913130063.

30. Magnoni M, Gallone G, Ceriotti F, et al. Prognostic implications of high-sensitivity cardiac troponin T assay in a real-world population with non-ST-elevation acute coronary syndrome. *IJC Hear Vasc*. 2018;20:14-19. doi:10.1016/j.ijcha.2018.06.004.

31. van der Linden N, Wildi K, Twerenbold R, et al. Combining High Sensitivity Cardiac Troponin I and Cardiac Troponin T in the Early Diagnosis of Acute Myocardial Infarction. *Circulation*. 2018;347(July):CIRCULATIONAHA.117.032003. doi:10.1161/CIRCULATIONAHA.117.032003.

32. Keller T, Zeller T, Peetz D, et al. Sensitive Troponin I Assay in Early Diagnosis of Acute Myocardial Infarction. *N Engl J Med*. 2009;361(9):868-877. doi:10.1056/NEJMoa0903515.

33. Möckel M, Landmesser U. Challenges in using high-sensitive troponin reporting in clinical practice—The important role of appropriate use in the context of

clinical evaluation. *Int J Cardiol*. 2017;245:61-62. doi:10.1016/j.ijcard.2017.07.019.

34. Pan BT, Johnstone RM. Fate of the transferrin receptor during maturation of sheep reticulocytes in vitro: Selective externalization of the receptor. *Cell*. 1983;33(3):967-978. doi:10.1016/0092-8674(83)90040-5.

35. Harding C, Heuser J, Stahl P. Receptor-mediated Endocytosis of Transferrin and of the Transferrin Receptor in Rat Reticulocytes Recycling. *J Cell Biol*. 1983;97:329-339. doi:10.1038/nrm973.

36. Johnstone RM, Adam M, Hammond JR, Orr L, Turbide C. Vesicle formation during reticulocyte maturation. Association of plasma membrane activities with released vesicles (exosomes). *J Biol Chem*. 1987;262(19):9412-9420. doi:10.1016/j.biocel.2011.10.005.

37. Raposo G, Nijman HW, Stoorvogel W, et al. B lymphocytes secrete antigen-presenting vesicles. *J Exp Med*. 1996;183(3):1161-72. doi:10.1088/1751-8113/44/8/085201.

38. Zitvogel L, Regnault A, Lozier A, et al. Eradication of established murine tumors using a novel cell-free vaccine: Dendritic cell-derived exosomes. *Nat Med*. 1998;4(5):594-600. doi:10.1038/nm0598-594.

39. Valadi H, Ekström K, Bossios A, Sjöstrand M, Lee JJ, Lötvall JO. Exosome-mediated transfer of mRNAs and microRNAs is a novel mechanism of genetic exchange between cells. *Nat Cell Biol*. 2007;9(6):654-659. doi:10.1038/ncb1596.

40. Colombo M, Raposo G, Théry C. Biogenesis, secretion, and intercellular interactions of exosomes and other extracellular vesicles. *Annu Rev Cell Dev Biol*. 2014;30(1):255-89. doi:10.1146/annurev-cellbio-101512-122326.

41. Lötvall J, Hill AF, Hochberg F, et al. Minimal experimental requirements for definition of extracellular vesicles and their functions: a position statement from the International Society for Extracellular Vesicles. *J Extracell vesicles*. 2014;3(1):26913. doi:10.3402/jev.v3.26913.

42. Ha D, Yang N, Nadithe V. Exosomes as therapeutic drug carriers and delivery vehicles across biological membranes: current perspectives and future challenges. *Acta Pharm Sin B*. 2016;6(4):287-296. doi:10.1016/j.apsb.2016.02.001.

43. Fiore EJ, Domínguez LM, Bayo J, García MG, Mazzolini GD. Taking advantage of the potential of mesenchymal stromal cells in liver regeneration: Cells and

extracellular vesicles as therapeutic strategies. *World J Gastroenterol*. 2018;24(23):2427-2440. doi:10.3748/wjg.v24.i23.2427.

44. Crescitelli R, Lässer C, Szabó TG, et al. Distinct RNA profiles in subpopulations of extracellular vesicles: apoptotic bodies, microvesicles and exosomes. *J Extracell vesicles*. 2013;2(1). doi:10.3402/jev.v2i0.20677.

45. Schiller M, Bekeredjian-Ding I, Heyder P, Blank N, Ho AD, Lorenz H-M. Autoantigens are translocated into small apoptotic bodies during early stages of apoptosis. *Cell Death Differ*. 2008;15(1):183-91. doi:10.1038/sj.cdd.4402239.

46. Than UTT, Guanzon D, Leavesley D, Parker T. Association of Extracellular Membrane Vesicles with Cutaneous Wound Healing. *Int J Mol Sci*. 2017;18(5):956. doi:10.3390/ijms18050956.

47. Cocucci E, Racchetti G, Meldolesi J. Shedding microvesicles: artefacts no more. *Trends Cell Biol*. 2009;19(2):43-51. doi:10.1016/j.tcb.2008.11.003.

48. Théry C, Zitvogel L, Amigorena S. Exosomes: composition, biogenesis and function. *Nat Rev Immunol*. 2002;2(8):569-79. doi:10.1038/nri855.

49. Blazek AD, Paleo BJ, Weisleder N. Plasma Membrane Repair: A Central Process for Maintaining Cellular Homeostasis. *Physiology*. 2015;30(6):438-448. doi:10.1152/physiol.00019.2015.

50. Andrews NW, Almeida PE, Corrotte M. Damage control: cellular mechanisms of plasma membrane repair. *Trends Cell Biol*. 2014;24(12):734-742. doi:10.1016/j.tcb.2014.07.008.

51. EL Andaloussi S, Mäger I, Breakefield XO, Wood MJA. Extracellular vesicles: biology and emerging therapeutic opportunities. *Nat Rev Drug Discov*. 2013;12(5):347-57. doi:10.1038/nrd3978.

52. Rajagopal C, Harikumar KB. The Origin and Functions of Exosomes in Cancer. *Front Oncol*. 2018;8(March):66. doi:10.3389/fonc.2018.00066.

53. Juan T, Fürthauer M. Biogenesis and function of ESCRT-dependent extracellular vesicles. *Semin Cell Dev Biol*. 2018;74:66-77. doi:10.1016/j.semcdb.2017.08.022.

54. Théry C, Ostrowski M, Segura E. Membrane vesicles as conveyors of immune responses. *Nat Rev Immunol*. 2009;9(8):581-93. doi:10.1038/nri2567.

55. Raposo G, Stoorvogel W. Extracellular vesicles: Exosomes, microvesicles, and friends. *J Cell Biol*. 2013;200(4):373-383. doi:10.1083/jcb.201211138.

56. Rupaimoole R, Slack FJ. MicroRNA therapeutics: towards a new era for the management of cancer and other diseases. *Nat Rev Drug Discov*. 2017;16(3):203-222. doi:10.1038/nrd.2016.246.

57. Matsui M, Corey DR. Non-coding RNAs as drug targets. *Nat Rev Drug Discov*. 2017;16(3):167-179. doi:10.1038/nrd.2016.117.

58. Bernardo BC, Ooi JYY, Lin RCY, McMullen JR. miRNA therapeutics: a new class of drugs with potential therapeutic applications in the heart. *Future Med Chem*. 2015;7(13):1771-1792. doi:10.4155/fmc.15.107.

59. Carthew RW, Sontheimer EJ. Origins and Mechanisms of miRNAs and siRNAs. *Cell*. 2009;136(4):642-655. doi:10.1016/j.cell.2009.01.035.

60. Kalluri R. The Biology and Function of Exosomes in Cancer. *J Clin Invest*. 2016;4(2010):2362. doi:https://doi.org/10.1172/JCI81135.

61. Steinbichler TB, Dudás J, Riechelmann H, Skvortsova I-I. The role of exosomes in cancer metastasis. *Semin Cancer Biol*. 2017;44:170-181. doi:10.1016/j.semcancer.2017.02.006.

62. Zheng G, Huang R, Qiu G, et al. Mesenchymal stromal cell-derived extracellular vesicles: regenerative and immunomodulatory effects and potential applications in sepsis. *Cell Tissue Res*. 2018;1991(Caplan 1991). doi:10.1007/s00441-018-2871-5.

63. Nie W, Ma X, Yang C, et al. Human mesenchymal-stem-cells-derived exosomes are important in enhancing porcine islet resistance to hypoxia. *Xenotransplantation*. 2018;(April):e12405. doi:10.1111/xen.12405.

64. Kordelas L, Rebmann V, Ludwig A-K, et al. MSC-derived exosomes: a novel tool to treat therapy-refractory graft-versus-host disease. *Leukemia*. 2014;28(4):970-3. doi:10.1038/leu.2014.41.

65. Bellavia D, Raimondi L, Costa V, et al. Engineered exosomes: A new promise for the management of musculoskeletal diseases. *Biochim Biophys Acta - Gen Subj*. 2018;1862(9):1893-1901. doi:10.1016/j.bbagen.2018.06.003.

66. Mentkowski KI, Snitzer JD, Rusnak S, Lang JK. Therapeutic Potential of Engineered Extracellular Vesicles. *AAPS J*. 2018;20(3):50. doi:10.1208/s12248-018-0211-z.

67. Kojima R, Bojar D, Rizzi G, et al. Designer exosomes produced by implanted cells intracerebrally deliver therapeutic cargo for Parkinson's disease treatment.

Nat Commun. 2018;9(1):1305. doi:10.1038/s41467-018-03733-8.

68. Yang S, Wang D, Li J, et al. Predictive role of GSTP1-containing exosomes in chemotherapy-resistant breast cancer. *Gene*. 2017;623:5-14. doi:10.1016/j.gene.2017.04.031.

69. Limoni SK, Moghadam MF, Moazzeni SM, Gomari H, Salimi F. Engineered Exosomes for Targeted Transfer of siRNA to HER2 Positive Breast Cancer Cells. *Appl Biochem Biotechnol*. 2018. doi:10.1007/s12010-018-2813-4.

70. Kim MS, Haney MJ, Zhao Y, et al. Development of exosome-encapsulated paclitaxel to overcome MDR in cancer cells. *Nanomedicine Nanotechnology, Biol Med*. 2016;12(3):655-664. doi:10.1016/j.nano.2015.10.012.

71. Rabinowits G, Gerçel-Taylor C, Day JM, Taylor DD, Kloecker GH. Exosomal microRNA: a diagnostic marker for lung cancer. *Clin Lung Cancer*. 2009;10(1):42-6. doi:10.3816/CLC.2009.n.006.

72. Hornick NI, Huan J, Doron B, et al. Serum Exosome MicroRNA as a Minimally-Invasive Early Biomarker of AML. *Sci Rep*. 2015;5(1):11295. doi:10.1038/srep11295.

73. Lane RE, Korbie D, Hill MM, Trau M. Extracellular vesicles as circulating cancer biomarkers: opportunities and challenges. *Clin Transl Med*. 2018;7(1):14. doi:10.1186/s40169-018-0192-7.

74. Yamamoto CM, Murakami T, Oakes ML, et al. Uromodulin mRNA from Urinary Extracellular Vesicles Correlate to Kidney Function Decline in Type 2 Diabetes Mellitus. *Am J Nephrol*. 2018;47(5):283-291. doi:10.1159/000489129.

75. Xu W-C, Qian G, Liu A-Q, Li Y-Q, Zou H-Q. Urinary Extracellular Vesicle: A Potential Source of Early Diagnostic and Therapeutic Biomarker in Diabetic Kidney Disease. *Chin Med J (Engl)*. 2018;131(11):1357. doi:10.4103/0366-6999.232801.

76. Dykes IM. Exosomes in Cardiovascular Medicine. *Cardiol Ther*. 2017;6(2):225-237. doi:10.1007/s40119-017-0091-9.

77. Ko J, Bhagwat N, Black T, et al. miRNA profiling of magnetic nanopore-isolated extracellular vesicles for the diagnosis of pancreatic cancer. *Cancer Res*. 2018:canres.3703.2017. doi:10.1158/0008-5472.CAN-17-3703.

78. Yang J, Li C, Zhang L, Wang X. Extracellular Vesicles as Carriers of Non-coding RNAs in Liver Diseases. *Front Pharmacol*. 2018;9(APR):1-11.

doi:10.3389/fphar.2018.00415.

79. Pomatto MAC, Gai C, Deregibus MC, Tetta C, Camussi G. Noncoding RNAs Carried by Extracellular Vesicles in Endocrine Diseases. *Int J Endocrinol*. 2018;2018:1-18. doi:10.1155/2018/4302096.

80. Bryant RJ, Pawlowski T, Catto JWF, et al. Changes in circulating microRNA levels associated with prostate cancer. *Br J Cancer*. 2012;106(4):768-774. doi:10.1038/bjc.2011.595.

81. Mitchell PS, Parkin RK, Kroh EM, et al. Circulating microRNAs as stable blood-based markers for cancer detection. *Proc Natl Acad Sci*. 2008;105(30):10513-10518. doi:10.1073/pnas.0804549105.

82. Konoshenko MY, Lekchnov EA, Vlassov A V., Laktionov PP. Isolation of Extracellular Vesicles: General Methodologies and Latest Trends. *Biomed Res Int*. 2018;2018:1-27. doi:10.1155/2018/8545347.

83. Lane RE, Korbie D, Trau M, Hill MM. Purification Protocols for Extracellular Vesicles. In: Kuo WP, Jia S, eds.Vol 1660. Methods in Molecular Biology. New York, NY: Springer New York; 2017:111-130. doi:10.1007/978-1-4939-7253-1_10.

84. van der Pol E, Boing AN, Harrison P, Sturk A, Nieuwland R. Classification, Functions, and Clinical Relevance of Extracellular Vesicles. *Pharmacol Rev*. 2012;64(3):676-705. doi:10.1124/pr.112.005983.

85. Gould SJ, Raposo G. As we wait: coping with an imperfect nomenclature for extracellular vesicles. *J Extracell Vesicles*. 2013;2(1):20389. doi:10.3402/jev.v2i0.20389.

86. Théry C, Amigorena S, Raposo G, Clayton A. Isolation and Characterization of Exosomes from Cell Culture Supernatants and Biological Fluids. *Curr Protoc Cell Biol*. 2006;30(1):3.22.1-3.22.29. doi:10.1002/0471143030.cb0322s30.

87. Coumans FAW, Brisson AR, Buzas EI, et al. Methodological Guidelines to Study Extracellular Vesicles. *Circ Res*. 2017;120(10):1632-1648. doi:10.1161/CIRCRESAHA.117.309417.

88. Willms E, Johansson HJ, Mäger I, et al. Cells release subpopulations of exosomes with distinct molecular and biological properties. *Sci Rep*. 2016;6(1):22519. doi:10.1038/srep22519.

89. Böing AN, van der Pol E, Grootemaat AE, Coumans FAW, Sturk A, Nieuwland

R. Single-step isolation of extracellular vesicles by size-exclusion chromatography. *J Extracell Vesicles*. 2014;3(1):23430. doi:10.3402/jev.v3.23430.

90. Cheruvanky A, Zhou H, Pisitkun T, et al. Rapid isolation of urinary exosomal biomarkers using a nanomembrane ultrafiltration concentrator. *Am J Physiol Physiol*. 2007;292(5):F1657-F1661. doi:10.1152/ajprenal.00434.2006.

91. Witwer KW, Buzás EI, Bemis LT, et al. Standardization of sample collection, isolation and analysis methods in extracellular vesicle research. *J Extracell Vesicles*. 2013;2(1):20360. doi:10.3402/jev.v2i0.20360.

92. Oksvold MP, Neurauter A, Pedersen KW. Magnetic Bead-Based Isolation of Exosomes. In: *Methods in Molecular Biology*.Vol 1218.; 2015:465-481. doi:10.1007/978-1-4939-1538-5_27.

93. Van Deun J, Mestdagh P, Sormunen R, et al. The impact of disparate isolation methods for extracellular vesicles on downstream RNA profiling. *J Extracell Vesicles*. 2014;3(1):24858. doi:10.3402/jev.v3.24858.

94. Liu Z, Cauvi DM, Bernardino EMA, et al. Isolation and characterization of human urine extracellular vesicles. *Cell Stress Chaperones*. 2018. doi:10.1007/s12192-018-0902-5.

95. Buschmann D, Kirchner B, Hermann S, et al. Evaluation of serum extracellular vesicle isolation methods for profiling miRNAs by next-generation sequencing. *J Extracell vesicles*. 2018;7(1):1481321. doi:10.1080/20013078.2018.1481321.

96. Yu Y, Gool E, Berckmans RJ, et al. Extracellular vesicles from human saliva promote hemostasis by delivering coagulant tissue factor to activated platelets. *J Thromb Haemost*. 2018;16(6):1153-1163. doi:10.1111/jth.14023.

97. Wang X. Isolation of Extracellular Vesicles from Breast Milk. In: Kuo WP, Jia S, eds.Vol 1660. Methods in Molecular Biology. New York, NY: Springer New York; 2017:351-353. doi:10.1007/978-1-4939-7253-1_28.

98. Yáñez-Mó M, Siljander PRM, Andreu Z, et al. Biological properties of extracellular vesicles and their physiological functions. *J Extracell vesicles*. 2015;4(2015):27066. doi:10.3402/jev.v4.27066.

99. Puhka M, Nordberg M-E, Valkonen S, et al. KeepEX, a simple dilution protocol for improving extracellular vesicle yields from urine. *Eur J Pharm Sci*. 2017;98:30-39. doi:10.1016/j.ejps.2016.10.021.

100. Li M, Zeringer E, Barta T, Schageman J, Cheng A, Vlassov A V. Analysis of the RNA content of the exosomes derived from blood serum and urine and its potential as biomarkers. *Philos Trans R Soc B Biol Sci*. 2014;369(1652):20130502-20130502. doi:10.1098/rstb.2013.0502.

101. Erdbrugger U, Le TH. Extracellular Vesicles in Renal Diseases: More than Novel Biomarkers? *J Am Soc Nephrol*. 2016;27(1):12-26. doi:10.1681/ASN.2015010074.

102. Musante L, Tataruch DE, Holthofer H. Use and Isolation of Urinary Exosomes as Biomarkers for Diabetic Nephropathy. *Front Endocrinol (Lausanne)*. 2014;5(SEP):1-13. doi:10.3389/fendo.2014.00149.

103. Pisitkun T, Shen R-F, Knepper MA. Identification and proteomic profiling of exosomes in human urine. *Proc Natl Acad Sci U S A*. 2004;101(36):13368-73. doi:10.1073/pnas.0403453101.

104. TAMM I, HORSFALL FL. Characterization and separation of an inhibitor of viral hemagglutination present in urine. *Proc Soc Exp Biol Med*. 1950;74(1):106-8. Available at: http://www.ncbi.nlm.nih.gov/pubmed/15430405.

105. Kobayashi K, Fukuoka S. Conditions for Solubilization of Tamm–Horsfall Protein/Uromodulin in Human Urine and Establishment of a Sensitive and Accurate Enzyme-Linked Immunosorbent Assay (ELISA) Method. *Arch Biochem Biophys*. 2001;388(1):113-120. doi:10.1006/abbi.2000.2265.

106. PHILLIPS F, KACZOR K, GANDHI N, et al. Measurement of sodium ion concentration in undiluted urine with cation-selective polymeric membrane electrodes after the removal of interfering compounds. *Talanta*. 2007;74(2):255-264. doi:10.1016/j.talanta.2007.06.011.

107. Fernández-Llama P, Khositseth S, Gonzales PA, Star RA, Pisitkun T, Knepper MA. Tamm-Horsfall protein and urinary exosome isolation. *Kidney Int*. 2010;77(8):736-742. doi:10.1038/ki.2009.550.

108. Cheng Y, Wang X, Yang J, et al. A translational study of urine miRNAs in acute myocardial infarction. *J Mol Cell Cardiol*. 2012;53(5):668-676. doi:10.1016/j.yjmcc.2012.08.010.

109. Street JM, Koritzinsky EH, Glispie DM, Yuen PST. Urine Exosome Isolation and Characterization. In: Gautier J-C, ed.Vol 1641. Methods in Molecular Biology. New York, NY: Springer New York; 2017:413-423. doi:10.1007/978-1-4939-7172-5_23.

110. Gąsecka A, van der Pol E, Nieuwland R, Stępień E. Extracellular vesicles in post-infarct ventricular remodelling. *Kardiol Pol*. 2018;76(1):69-76. doi:10.5603/KP.a2017.0178.

111. Van Deun J, Mestdagh P, Agostinis P, et al. EV-TRACK: transparent reporting and centralizing knowledge in extracellular vesicle research. *Nat Methods*. 2017;14(3):228-232. doi:10.1038/nmeth.4185.

112. Webber J, Clayton A. How pure are your vesicles? *J Extracell Vesicles*. 2013;2(1):19861. doi:10.3402/jev.v2i0.19861.

113. Pisitkun T, Shen R-F, Knepper MA. Identification and proteomic profiling of exosomes in human urine. *Proc Natl Acad Sci*. 2004;101(36):13368-13373. doi:10.1073/pnas.0403453101.

114. Bokhove M, Nishimura K, Brunati M, et al. A structured interdomain linker directs self-polymerization of human uromodulin. *Proc Natl Acad Sci*. 2016;113(6):1552-1557. doi:10.1073/pnas.1519803113.

115. Morales-Kastresana A, Telford B, Musich TA, et al. Labeling Extracellular Vesicles for Nanoscale Flow Cytometry. *Sci Rep*. 2017;7(1):1878. doi:10.1038/s41598-017-01731-2.

116. Nair R, Santos L, Awasthi S, et al. Extracellular Vesicles Derived from Preosteoblasts Influence Embryonic Stem Cell Differentiation. *Stem Cells Dev*. 2014;23(14):1625-1635. doi:10.1089/scd.2013.0633.

117. van der Vlist EJ, Nolte-'t Hoen ENM, Stoorvogel W, Arkesteijn GJA, Wauben MHM. Fluorescent labeling of nano-sized vesicles released by cells and subsequent quantitative and qualitative analysis by high-resolution flow cytometry. *Nat Protoc*. 2012;7(7):1311-1326. doi:10.1038/nprot.2012.065.

118. Ratajczak MZ, Kucia M, Jadczyk T, et al. Pivotal role of paracrine effects in stem cell therapies in regenerative medicine: can we translate stem cell-secreted paracrine factors and microvesicles into better therapeutic strategies? *Leukemia*. 2012;26(6):1166-1173. doi:10.1038/leu.2011.389.

119. Boos CJ, Lip GYH, Blann AD. Circulating Endothelial Cells in Cardiovascular Disease. *J Am Coll Cardiol*. 2006;48(8):1538-1547. doi:10.1016/j.jacc.2006.02.078.

120. Madden JA. Role of the vascular endothelium and plaque in acute ischemic stroke. *Neurology*. 2012;79(Issue 13, Supplement 1):S58-S62. doi:10.1212/WNL.0b013e3182695836.

121. Erbs S, Linke A, Schachinger V, et al. Restoration of Microvascular Function in the Infarct-Related Artery by Intracoronary Transplantation of Bone Marrow Progenitor Cells in Patients With Acute Myocardial Infarction: The Doppler Substudy of the Reinfusion of Enriched Progenitor Cells and Infa. *Circulation*. 2007;116(4):366-374. doi:10.1161/CIRCULATIONAHA.106.671545.

122. Gupta R, Tongers J, Losordo DW. Human Studies of Angiogenic Gene Therapy. *Circ Res*. 2009;105(8):724-736. doi:10.1161/CIRCRESAHA.109.200386.

123. Badimon L, Borrell M. Microvasculature recovery by angiogenesis after myocardial infarction. *Curr Pharm Des*. 2018;24. doi:10.2174/1381612824666180629162726.

124. Velagapudi P, Turagam M, Kolte D, et al. Intramyocardial autologous CD34+ cell therapy for refractory angina: A meta-analysis of randomized controlled trials. *Cardiovasc Revascularization Med*. 2018:1-5. doi:10.1016/j.carrev.2018.05.018.

125. Potz BA, Scrimgeour LA, Pavlov VI, Sodha NR, Abid MR, Sellke FW. Extracellular Vesicle Injection Improves Myocardial Function and Increases Angiogenesis in a Swine Model of Chronic Ischemia. *J Am Heart Assoc*. 2018;7(12):e008344. doi:10.1161/JAHA.117.008344.

126. Nowak-Sliwinska P, Alitalo K, Allen E, et al. Consensus guidelines for the use and interpretation of angiogenesis assays. *Angiogenesis*. 2018;(0123456789):1-108. doi:10.1007/s10456-018-9613-x.

127. Ronco C, Haapio M, House AA, Anavekar N, Bellomo R. Cardiorenal Syndrome. *J Am Coll Cardiol*. 2008;52(19):1527-1539. doi:10.1016/j.jacc.2008.07.051.

128. Kanic V, Vollrath M, Kompara G, Suran D, Hojs R. Women and acute kidney injury in myocardial infarction. *J Nephrol*. 2018;0(0):0. doi:10.1007/s40620-018-0504-4.

129. Christensson A, Melander O, Fjellstedt E, Ohlson-Andersson M. Family History of Myocardial Infarction Increases Risk of Renal Dysfunction in Middle Age. *Am J Nephrol*. 2014;39(2):85-91. doi:10.1159/000358259.

130. Liu Q, Rojas-Canales DM, Divito SJ, et al. Donor dendritic cell–derived exosomes promote allograft-targeting immune response. *J Clin Invest*. 2016;126(8):2805-2820. doi:10.1172/JCI84577.

8. Annex

8.1. Statistical analysis of "Cell media optimization for bioactivity assays" experiment

8.1.1. PrestoBlue™ measurement at 24 hours:

Table 3 – Statistical analysis of PrestoBlue™ measurement at 24 hours.

Number of families	1			
Number of comparisons per family	91			
Alpha	0,05			
Tukey's multiple comparisons test	Mean Diff,	95% CI of diff,	Significant?	Summary
EBM vs. EBM + VEGF	-740,9	-1048 to -433,9	Yes	****
EBM vs. EBM + 0.1% FBS	-417,9	-724,8 to -110,9	Yes	***
EBM vs. EBM + 0.1% FBS + VEGF	-1012	-1319 to -704,8	Yes	****
EBM vs. EBM + 1% FBS	-913,3	-1220 to -606,4	Yes	****
EBM vs. EBM + 1% FBS + VEGF	-1275	-1582 to -968,5	Yes	****
EBM vs. EBM + 2% FBS	-1168	-1475 to -861,5	Yes	****
EBM vs. EBM + 2% FBS + VEGF	-1392	-1699 to -1085	Yes	****
EBM vs. EBM + 5% FBS	-1405	-1712 to -1098	Yes	****
EBM vs. EBM + 5% FBS + VEGF	-1734	-2041 to -1427	Yes	****
EBM vs. EBM + 10% FBS	-1406	-1713 to -1099	Yes	****
EBM vs. EBM + 10% FBS + VEGF	-2078	-2385 to -1771	Yes	****
EBM vs. EGM-2	-2246	-2565 to -1926	Yes	****
EBM vs. EGM-2 + VEGF	-2468	-2788 to -2149	Yes	****
EBM + VEGF vs. EBM + 0.1% FBS	323	16,08 to 629,9	Yes	*
EBM + VEGF vs. EBM + 0.1% FBS + VEGF	-270,9	-577,8 to 36,06	No	ns
EBM + VEGF vs. EBM + 1% FBS	-172,4	-479,3 to 134,5	No	ns
EBM + VEGF vs. EBM + 1% FBS + VEGF	-534,6	-841,5 to -227,7	Yes	****
EBM + VEGF vs. EBM + 2% FBS	-427,6	-734,5 to -120,7	Yes	***
EBM + VEGF vs. EBM + 2% FBS + VEGF	-651,3	-958,2 to -344,4	Yes	****
EBM + VEGF vs. EBM + 5% FBS	-664,4	-971,3 to -357,5	Yes	****
EBM + VEGF vs. EBM + 5% FBS + VEGF	-992,9	-1300 to -685,9	Yes	****

EBM + VEGF vs. EBM + 10% FBS	-665,3	-972,2 to -358,4	Yes	****
EBM + VEGF vs. EBM + 10% FBS + VEGF	-1337	-1644 to -1030	Yes	****
EBM + VEGF vs. EGM-2	-1505	-1824 to -1185	Yes	****
EBM + VEGF vs. EGM-2 + VEGF	-1727	-2047 to -1408	Yes	****
EBM + 0.1% FBS vs. EBM + 0.1% FBS + VEGF	-593,9	-900,8 to -286,9	Yes	****
EBM + 0.1% FBS vs. EBM + 1% FBS	-495,4	-802,3 to -188,5	Yes	****
EBM + 0.1% FBS vs. EBM + 1% FBS + VEGF	-857,6	-1164 to -550,7	Yes	****
EBM + 0.1% FBS vs. EBM + 2% FBS	-750,6	-1057 to -443,7	Yes	****
EBM + 0.1% FBS vs. EBM + 2% FBS + VEGF	-974,3	-1281 to -667,4	Yes	****
EBM + 0.1% FBS vs. EBM + 5% FBS	-987,4	-1294 to -680,5	Yes	****
EBM + 0.1% FBS vs. EBM + 5% FBS + VEGF	-1316	-1623 to -1009	Yes	****
EBM + 0.1% FBS vs. EBM + 10% FBS	-988,3	-1295 to -681,4	Yes	****
EBM + 0.1% FBS vs. EBM + 10% FBS + VEGF	-1660	-1967 to -1353	Yes	****
EBM + 0.1% FBS vs. EGM-2	-1828	-2147 to -1508	Yes	****
EBM + 0.1% FBS vs. EGM-2 + VEGF	-2050	-2370 to -1731	Yes	****
EBM + 0.1% FBS + VEGF vs. EBM + 1% FBS	98,43	-208,5 to 405,3	No	ns
EBM + 0.1% FBS + VEGF vs. EBM + 1% FBS + VEGF	-263,7	-570,6 to 43,20	No	ns
EBM + 0.1% FBS + VEGF vs. EBM + 2% FBS	-156,7	-463,6 to 150,2	No	ns
EBM + 0.1% FBS + VEGF vs. EBM + 2% FBS + VEGF	-380,4	-687,3 to -73,51	Yes	**
EBM + 0.1% FBS + VEGF vs. EBM + 5% FBS	-393,6	-700,5 to -86,66	Yes	**
EBM + 0.1% FBS + VEGF vs. EBM + 5% FBS + VEGF	-722	-1029 to -415,1	Yes	****
EBM + 0.1% FBS + VEGF vs. EBM + 10% FBS	-394,4	-701,3 to -87,51	Yes	**
EBM + 0.1% FBS + VEGF vs. EBM + 10% FBS + VEGF	-1066	-1373 to -759,1	Yes	****
EBM + 0.1% FBS + VEGF vs. EGM-2	-1234	-1553 to -914,6	Yes	****
EBM + 0.1% FBS + VEGF vs. EGM-2 + VEGF	-1457	-1776 to -1137	Yes	****
EBM + 1% FBS vs. EBM + 1% FBS + VEGF	-362,1	-669,1 to -55,23	Yes	**
EBM + 1% FBS vs. EBM + 2% FBS	-255,1	-562,1 to 51,77	No	ns
EBM + 1% FBS vs. EBM + 2% FBS + VEGF	-478,9	-785,8 to -171,9	Yes	****
EBM + 1% FBS vs. EBM + 5% FBS	-492	-798,9 to -185,1	Yes	****
EBM + 1% FBS vs. EBM + 5% FBS + VEGF	-820,4	-1127 to -513,5	Yes	****

EBM + 1% FBS vs. EBM + 10% FBS	-492,9	-799,8 to -185,9	Yes	****
EBM + 1% FBS vs. EBM + 10% FBS + VEGF	-1164	-1471 to -857,5	Yes	****
EBM + 1% FBS vs. EGM-2	-1332	-1652 to -1013	Yes	****
EBM + 1% FBS vs. EGM-2 + VEGF	-1555	-1874 to -1236	Yes	****
EBM + 1% FBS + VEGF vs. EBM + 2% FBS	107	-199,9 to 413,9	No	ns
EBM + 1% FBS + VEGF vs. EBM + 2% FBS + VEGF	-116,7	-423,6 to 190,2	No	ns
EBM + 1% FBS + VEGF vs. EBM + 5% FBS	-129,9	-436,8 to 177,1	No	ns
EBM + 1% FBS + VEGF vs. EBM + 5% FBS + VEGF	-458,3	-765,2 to -151,4	Yes	***
EBM + 1% FBS + VEGF vs. EBM + 10% FBS	-130,7	-437,6 to 176,2	No	ns
EBM + 1% FBS + VEGF vs. EBM + 10% FBS + VEGF	-802,3	-1109 to -495,4	Yes	****
EBM + 1% FBS + VEGF vs. EGM-2	-970,3	-1290 to -650,9	Yes	****
EBM + 1% FBS + VEGF vs. EGM-2 + VEGF	-1193	-1512 to -873,4	Yes	****
EBM + 2% FBS vs. EBM + 2% FBS + VEGF	-223,7	-530,6 to 83,20	No	ns
EBM + 2% FBS vs. EBM + 5% FBS	-236,9	-543,8 to 70,06	No	ns
EBM + 2% FBS vs. EBM + 5% FBS + VEGF	-565,3	-872,2 to -258,4	Yes	****
EBM + 2% FBS vs. EBM + 10% FBS	-237,7	-544,6 to 69,20	No	ns
EBM + 2% FBS vs. EBM + 10% FBS + VEGF	-909,3	-1216 to -602,4	Yes	****
EBM + 2% FBS vs. EGM-2	-1077	-1397 to -757,9	Yes	****
EBM + 2% FBS vs. EGM-2 + VEGF	-1300	-1619 to -980,4	Yes	****
EBM + 2% FBS + VEGF vs. EBM + 5% FBS	-13,14	-320,1 to 293,8	No	ns
EBM + 2% FBS + VEGF vs. EBM + 5% FBS + VEGF	-341,6	-648,5 to -34,66	Yes	*
EBM + 2% FBS + VEGF vs. EBM + 10% FBS	-14	-320,9 to 292,9	No	ns
EBM + 2% FBS + VEGF vs. EBM + 10% FBS + VEGF	-685,6	-992,5 to -378,7	Yes	****
EBM + 2% FBS + VEGF vs. EGM-2	-853,6	-1173 to -534,1	Yes	****
EBM + 2% FBS + VEGF vs. EGM-2 + VEGF	-1076	-1396 to -756,6	Yes	****
EBM + 5% FBS vs. EBM + 5% FBS + VEGF	-328,4	-635,3 to -21,51	Yes	*
EBM + 5% FBS vs. EBM + 10% FBS	-0,8571	-307,8 to 306,1	No	ns
EBM + 5% FBS vs. EBM + 10% FBS + VEGF	-672,4	-979,3 to -365,5	Yes	****
EBM + 5% FBS vs. EGM-2	-840,5	-1160 to -521,0	Yes	****
EBM + 5% FBS vs. EGM-2 + VEGF	-1063	-1382 to -743,5	Yes	****

EBM + 5% FBS + VEGF vs. EBM + 10% FBS	327,6	20,66 to 634,5	Yes	*
EBM + 5% FBS + VEGF vs. EBM + 10% FBS + VEGF	-344	-650,9 to -37,08	Yes	*
EBM + 5% FBS + VEGF vs. EGM-2	-512	-831,5 to -192,6	Yes	****
EBM + 5% FBS + VEGF vs. EGM-2 + VEGF	-734,5	-1054 to -415,1	Yes	****
EBM + 10% FBS vs. EBM + 10% FBS + VEGF	-671,6	-978,5 to -364,7	Yes	****
EBM + 10% FBS vs. EGM-2	-839,6	-1159 to -520,1	Yes	****
EBM + 10% FBS vs. EGM-2 + VEGF	-1062	-1382 to -742,6	Yes	****
EBM + 10% FBS + VEGF vs. EGM-2	-168	-487,5 to 151,4	No	ns
EBM + 10% FBS + VEGF vs. EGM-2 + VEGF	-390,5	-710,0 to -71,08	Yes	**
EGM-2 vs. EGM-2 + VEGF	-222,5	-554,0 to 109,0	No	ns

8.1.2. PrestoBlueTM measurement at 48 hours:

Table 4 – Statistical analysis of PrestoBlue^{TM} measurement at 48 hours.

Number of families	1			
Number of comparisons per family	91			
Alpha	0,05			
Tukey's multiple comparisons test	Mean Diff,	95% CI of diff,	Significant?	Summary
EBM vs. EBM + VEGF	-594,9	-897,4 to -292,3	Yes	****
EBM vs. EBM + 0.1% FBS	-508	-810,6 to -205,4	Yes	****
EBM vs. EBM + 0.1% FBS + VEGF	-1111	-1414 to -808,4	Yes	****
EBM vs. EBM + 1% FBS	-1220	-1522 to -917,0	Yes	****
EBM vs. EBM + 1% FBS + VEGF	-1810	-2112 to -1507	Yes	****
EBM vs. EBM + 2% FBS	-1929	-2232 to -1627	Yes	****
EBM vs. EBM + 2% FBS + VEGF	-2052	-2354 to -1749	Yes	****
EBM vs. EBM + 5% FBS	-2633	-2935 to -2330	Yes	****
EBM vs. EBM + 5% FBS + VEGF	-2695	-2998 to -2393	Yes	****
EBM vs. EBM + 10% FBS	-2953	-3255 to -2650	Yes	****
EBM vs. EBM + 10% FBS + VEGF	-3208	-3510 to -2905	Yes	****
EBM vs. EGM-2	-3484	-3799 to -3169	Yes	****
EBM vs. EGM-2 + VEGF	-3724	-4039 to -3409	Yes	****
EBM + VEGF vs. EBM + 0.1%	86,86	-215,7 to	No	ns

FBS		389,4		
EBM + VEGF vs. EBM + 0.1% FBS + VEGF	-516,1	-818,7 to -213,6	Yes	****
EBM + VEGF vs. EBM + 1% FBS	-624,7	-927,3 to -322,1	Yes	****
EBM + VEGF vs. EBM + 1% FBS + VEGF	-1215	-1518 to -912,4	Yes	****
EBM + VEGF vs. EBM + 2% FBS	-1334	-1637 to -1032	Yes	****
EBM + VEGF vs. EBM + 2% FBS + VEGF	-1457	-1760 to -1154	Yes	****
EBM + VEGF vs. EBM + 5% FBS	-2038	-2340 to -1735	Yes	****
EBM + VEGF vs. EBM + 5% FBS + VEGF	-2101	-2403 to -1798	Yes	****
EBM + VEGF vs. EBM + 10% FBS	-2358	-2660 to -2055	Yes	****
EBM + VEGF vs. EBM + 10% FBS + VEGF	-2613	-2916 to -2310	Yes	****
EBM + VEGF vs. EGM-2	-2889	-3204 to -2574	Yes	****
EBM + VEGF vs. EGM-2 + VEGF	-3129	-3444 to -2814	Yes	****
EBM + 0.1% FBS vs. EBM + 0.1% FBS + VEGF	-603	-905,6 to -300,4	Yes	****
EBM + 0.1% FBS vs. EBM + 1% FBS	-711,6	-1014 to -409,0	Yes	****
EBM + 0.1% FBS vs. EBM + 1% FBS + VEGF	-1302	-1604 to -999,3	Yes	****
EBM + 0.1% FBS vs. EBM + 2% FBS	-1421	-1724 to -1119	Yes	****
EBM + 0.1% FBS vs. EBM + 2% FBS + VEGF	-1544	-1846 to -1241	Yes	****
EBM + 0.1% FBS vs. EBM + 5% FBS	-2125	-2427 to -1822	Yes	****
EBM + 0.1% FBS vs. EBM + 5% FBS + VEGF	-2187	-2490 to -1885	Yes	****
EBM + 0.1% FBS vs. EBM + 10% FBS	-2445	-2747 to -2142	Yes	****
EBM + 0.1% FBS vs. EBM + 10% FBS + VEGF	-2700	-3002 to -2397	Yes	****
EBM + 0.1% FBS vs. EGM-2	-2976	-3291 to -2661	Yes	****
EBM + 0.1% FBS vs. EGM-2 + VEGF	-3216	-3531 to -2901	Yes	****
EBM + 0.1% FBS + VEGF vs. EBM + 1% FBS	-108,6	-411,2 to 194,0	No	ns
EBM + 0.1% FBS + VEGF vs. EBM + 1% FBS + VEGF	-698,9	-1001 to -396,3	Yes	****
EBM + 0.1% FBS + VEGF vs. EBM + 2% FBS	-818,3	-1121 to -515,7	Yes	****
EBM + 0.1% FBS + VEGF vs. EBM + 2% FBS + VEGF	-940,9	-1243 to -638,3	Yes	****
EBM + 0.1% FBS + VEGF vs. EBM + 5% FBS	-1522	-1824 to -1219	Yes	****
EBM + 0.1% FBS + VEGF vs. EBM + 5% FBS + VEGF	-1584	-1887 to -1282	Yes	****
EBM + 0.1% FBS + VEGF vs. EBM + 10% FBS	-1842	-2144 to -1539	Yes	****
EBM + 0.1% FBS + VEGF vs.	-2097	-2399 to -1794	Yes	****

EBM + 10% FBS + VEGF				
EBM + 0.1% FBS + VEGF vs. EGM-2	-2373	-2688 to -2058	Yes	****
EBM + 0.1% FBS + VEGF vs. EGM-2 + VEGF	-2613	-2928 to -2298	Yes	****
EBM + 1% FBS vs. EBM + 1% FBS + VEGF	-590,3	-892,9 to -287,7	Yes	****
EBM + 1% FBS vs. EBM + 2% FBS	-709,7	-1012 to -407,1	Yes	****
EBM + 1% FBS vs. EBM + 2% FBS + VEGF	-832,3	-1135 to -529,7	Yes	****
EBM + 1% FBS vs. EBM + 5% FBS	-1413	-1716 to -1111	Yes	****
EBM + 1% FBS vs. EBM + 5% FBS + VEGF	-1476	-1778 to -1173	Yes	****
EBM + 1% FBS vs. EBM + 10% FBS	-1733	-2036 to -1431	Yes	****
EBM + 1% FBS vs. EBM + 10% FBS + VEGF	-1988	-2291 to -1686	Yes	****
EBM + 1% FBS vs. EGM-2	-2265	-2580 to -1950	Yes	****
EBM + 1% FBS vs. EGM-2 + VEGF	-2505	-2820 to -2190	Yes	****
EBM + 1% FBS + VEGF vs. EBM + 2% FBS	-119,4	-422,0 to 183,2	No	ns
EBM + 1% FBS + VEGF vs. EBM + 2% FBS + VEGF	-242	-544,6 to 60,58	No	ns
EBM + 1% FBS + VEGF vs. EBM + 5% FBS	-822,9	-1125 to -520,3	Yes	****
EBM + 1% FBS + VEGF vs. EBM + 5% FBS + VEGF	-885,6	-1188 to -583,0	Yes	****
EBM + 1% FBS + VEGF vs. EBM + 10% FBS	-1143	-1445 to -840,3	Yes	****
EBM + 1% FBS + VEGF vs. EBM + 10% FBS + VEGF	-1398	-1701 to -1095	Yes	****
EBM + 1% FBS + VEGF vs. EGM-2	-1674	-1989 to -1359	Yes	****
EBM + 1% FBS + VEGF vs. EGM-2 + VEGF	-1914	-2229 to -1599	Yes	****
EBM + 2% FBS vs. EBM + 2% FBS + VEGF	-122,6	-425,2 to 180,0	No	ns
EBM + 2% FBS vs. EBM + 5% FBS	-703,4	-1006 to -400,8	Yes	****
EBM + 2% FBS vs. EBM + 5% FBS + VEGF	-766,1	-1069 to -463,6	Yes	****
EBM + 2% FBS vs. EBM + 10% FBS	-1023	-1326 to -720,8	Yes	****
EBM + 2% FBS vs. EBM + 10% FBS + VEGF	-1279	-1581 to -976,0	Yes	****
EBM + 2% FBS vs. EGM-2	-1555	-1870 to -1240	Yes	****
EBM + 2% FBS vs. EGM-2 + VEGF	-1795	-2110 to -1480	Yes	****
EBM + 2% FBS + VEGF vs. EBM + 5% FBS	-580,9	-883,4 to -278,3	Yes	****
EBM + 2% FBS + VEGF vs. EBM + 5% FBS + VEGF	-643,6	-946,2 to -341,0	Yes	****
EBM + 2% FBS + VEGF vs. EBM + 10% FBS	-900,9	-1203 to -598,3	Yes	****
EBM + 2% FBS + VEGF vs.	-1156	-1459 to -	Yes	****

EBM + 10% FBS + VEGF		853,4		
EBM + 2% FBS + VEGF vs. EGM-2	-1432	-1747 to -1117	Yes	****
EBM + 2% FBS + VEGF vs. EGM-2 + VEGF	-1672	-1987 to -1357	Yes	****
EBM + 5% FBS vs. EBM + 5% FBS + VEGF	-62,71	-365,3 to 239,9	No	ns
EBM + 5% FBS vs. EBM + 10% FBS	-320	-622,6 to -17,42	Yes	*
EBM + 5% FBS vs. EBM + 10% FBS + VEGF	-575,1	-877,7 to -272,6	Yes	****
EBM + 5% FBS vs. EGM-2	-851,5	-1166 to -536,6	Yes	****
EBM + 5% FBS vs. EGM-2 + VEGF	-1092	-1406 to -776,6	Yes	****
EBM + 5% FBS + VEGF vs. EBM + 10% FBS	-257,3	-559,9 to 45,30	No	ns
EBM + 5% FBS + VEGF vs. EBM + 10% FBS + VEGF	-512,4	-815,0 to -209,8	Yes	****
EBM + 5% FBS + VEGF vs. EGM-2	-788,8	-1104 to -473,9	Yes	****
EBM + 5% FBS + VEGF vs. EGM-2 + VEGF	-1029	-1344 to -713,9	Yes	****
EBM + 10% FBS vs. EBM + 10% FBS + VEGF	-255,1	-557,7 to 47,44	No	ns
EBM + 10% FBS vs. EGM-2	-531,5	-846,5 to -216,6	Yes	****
EBM + 10% FBS vs. EGM-2 + VEGF	-771,5	-1086 to -456,6	Yes	****
EBM + 10% FBS + VEGF vs. EGM-2	-276,4	-591,3 to 38,54	No	ns
EBM + 10% FBS + VEGF vs. EGM-2 + VEGF	-516,4	-831,3 to -201,5	Yes	****
EGM-2 vs. EGM-2 + VEGF	-240	-566,8 to 86,83	No	ns

8.1.3. Cell number measurement at 48 hours:

Table 5 – Statistical analysis of cell number measurement at 48 hours.

Number of families	1			
Number of comparisons per family	91			
Alpha	0,05			
Tukey's multiple comparisons test	Mean Diff,	95% CI of diff,	Significant?	Summary
EBM vs. EBM + VEGF	-594,9	-897,4 to -292,3	Yes	****
EBM vs. EBM + 0.1% FBS	-508	-810,6 to -205,4	Yes	****
EBM vs. EBM + 0.1% FBS + VEGF	-1111	-1414 to -808,4	Yes	****
EBM vs. EBM + 1% FBS	-1220	-1522 to -917,0	Yes	****

EBM vs. EBM + 1% FBS + VEGF	-1810	-2112 to -1507	Yes	****
EBM vs. EBM + 2% FBS	-1929	-2232 to -1627	Yes	****
EBM vs. EBM + 2% FBS + VEGF	-2052	-2354 to -1749	Yes	****
EBM vs. EBM + 5% FBS	-2633	-2935 to -2330	Yes	****
EBM vs. EBM + 5% FBS + VEGF	-2695	-2998 to -2393	Yes	****
EBM vs. EBM + 10% FBS	-2953	-3255 to -2650	Yes	****
EBM vs. EBM + 10% FBS + VEGF	-3208	-3510 to -2905	Yes	****
EBM vs. EGM-2	-3484	-3799 to -3169	Yes	****
EBM vs. EGM-2 + VEGF	-3724	-4039 to -3409	Yes	****
EBM + VEGF vs. EBM + 0.1% FBS	86,86	-215,7 to 389,4	No	ns
EBM + VEGF vs. EBM + 0.1% FBS + VEGF	-516,1	-818,7 to -213,6	Yes	****
EBM + VEGF vs. EBM + 1% FBS	-624,7	-927,3 to -322,1	Yes	****
EBM + VEGF vs. EBM + 1% FBS + VEGF	-1215	-1518 to -912,4	Yes	****
EBM + VEGF vs. EBM + 2% FBS	-1334	-1637 to -1032	Yes	****
EBM + VEGF vs. EBM + 2% FBS + VEGF	-1457	-1760 to -1154	Yes	****
EBM + VEGF vs. EBM + 5% FBS	-2038	-2340 to -1735	Yes	****
EBM + VEGF vs. EBM + 5% FBS + VEGF	-2101	-2403 to -1798	Yes	****
EBM + VEGF vs. EBM + 10% FBS	-2358	-2660 to -2055	Yes	****
EBM + VEGF vs. EBM + 10% FBS + VEGF	-2613	-2916 to -2310	Yes	****
EBM + VEGF vs. EGM-2	-2889	-3204 to -2574	Yes	****
EBM + VEGF vs. EGM-2 + VEGF	-3129	-3444 to -2814	Yes	****
EBM + 0.1% FBS vs. EBM + 0.1% FBS + VEGF	-603	-905,6 to -300,4	Yes	****
EBM + 0.1% FBS vs. EBM + 1% FBS	-711,6	-1014 to -409,0	Yes	****
EBM + 0.1% FBS vs. EBM + 1% FBS + VEGF	-1302	-1604 to -999,3	Yes	****
EBM + 0.1% FBS vs. EBM + 2% FBS	-1421	-1724 to -1119	Yes	****
EBM + 0.1% FBS vs. EBM + 2% FBS + VEGF	-1544	-1846 to -1241	Yes	****
EBM + 0.1% FBS vs. EBM + 5% FBS	-2125	-2427 to -1822	Yes	****
EBM + 0.1% FBS vs. EBM + 5% FBS + VEGF	-2187	-2490 to -1885	Yes	****
EBM + 0.1% FBS vs. EBM + 10% FBS	-2445	-2747 to -2142	Yes	****
EBM + 0.1% FBS vs. EBM + 10% FBS + VEGF	-2700	-3002 to -2397	Yes	****
EBM + 0.1% FBS vs. EGM-2	-2976	-3291 to -2661	Yes	****
EBM + 0.1% FBS vs. EGM-2 + VEGF	-3216	-3531 to -2901	Yes	****

EBM + 0.1% FBS + VEGF vs. EBM + 1% FBS	-108,6	-411,2 to 194,0	No	ns
EBM + 0.1% FBS + VEGF vs. EBM + 1% FBS + VEGF	-698,9	-1001 to -396,3	Yes	****
EBM + 0.1% FBS + VEGF vs. EBM + 2% FBS	-818,3	-1121 to -515,7	Yes	****
EBM + 0.1% FBS + VEGF vs. EBM + 2% FBS + VEGF	-940,9	-1243 to -638,3	Yes	****
EBM + 0.1% FBS + VEGF vs. EBM + 5% FBS	-1522	-1824 to -1219	Yes	****
EBM + 0.1% FBS + VEGF vs. EBM + 5% FBS + VEGF	-1584	-1887 to -1282	Yes	****
EBM + 0.1% FBS + VEGF vs. EBM + 10% FBS	-1842	-2144 to -1539	Yes	****
EBM + 0.1% FBS + VEGF vs. EBM + 10% FBS + VEGF	-2097	-2399 to -1794	Yes	****
EBM + 0.1% FBS + VEGF vs. EGM-2	-2373	-2688 to -2058	Yes	****
EBM + 0.1% FBS + VEGF vs. EGM-2 + VEGF	-2613	-2928 to -2298	Yes	****
EBM + 1% FBS vs. EBM + 1% FBS + VEGF	-590,3	-892,9 to -287,7	Yes	****
EBM + 1% FBS vs. EBM + 2% FBS	-709,7	-1012 to -407,1	Yes	****
EBM + 1% FBS vs. EBM + 2% FBS + VEGF	-832,3	-1135 to -529,7	Yes	****
EBM + 1% FBS vs. EBM + 5% FBS	-1413	-1716 to -1111	Yes	****
EBM + 1% FBS vs. EBM + 5% FBS + VEGF	-1476	-1778 to -1173	Yes	****
EBM + 1% FBS vs. EBM + 10% FBS	-1733	-2036 to -1431	Yes	****
EBM + 1% FBS vs. EBM + 10% FBS + VEGF	-1988	-2291 to -1686	Yes	****
EBM + 1% FBS vs. EGM-2	-2265	-2580 to -1950	Yes	****
EBM + 1% FBS vs. EGM-2 + VEGF	-2505	-2820 to -2190	Yes	****
EBM + 1% FBS + VEGF vs. EBM + 2% FBS	-119,4	-422,0 to 183,2	No	ns
EBM + 1% FBS + VEGF vs. EBM + 2% FBS + VEGF	-242	-544,6 to 60,58	No	ns
EBM + 1% FBS + VEGF vs. EBM + 5% FBS	-822,9	-1125 to -520,3	Yes	****
EBM + 1% FBS + VEGF vs. EBM + 5% FBS + VEGF	-885,6	-1188 to -583,0	Yes	****
EBM + 1% FBS + VEGF vs. EBM + 10% FBS	-1143	-1445 to -840,3	Yes	****
EBM + 1% FBS + VEGF vs. EBM + 10% FBS + VEGF	-1398	-1701 to -1095	Yes	****
EBM + 1% FBS + VEGF vs. EGM-2	-1674	-1989 to -1359	Yes	****
EBM + 1% FBS + VEGF vs. EGM-2 + VEGF	-1914	-2229 to -1599	Yes	****
EBM + 2% FBS vs. EBM + 2% FBS + VEGF	-122,6	-425,2 to 180,0	No	ns
EBM + 2% FBS vs. EBM + 5% FBS	-703,4	-1006 to -400,8	Yes	****
EBM + 2% FBS vs. EBM + 5% FBS + VEGF	-766,1	-1069 to -463,6	Yes	****

EBM + 2% FBS vs. EBM + 10% FBS	-1023	-1326 to -720,8	Yes	****
EBM + 2% FBS vs. EBM + 10% FBS + VEGF	-1279	-1581 to -976,0	Yes	****
EBM + 2% FBS vs. EGM-2	-1555	-1870 to -1240	Yes	****
EBM + 2% FBS vs. EGM-2 + VEGF	-1795	-2110 to -1480	Yes	****
EBM + 2% FBS + VEGF vs. EBM + 5% FBS	-580,9	-883,4 to -278,3	Yes	****
EBM + 2% FBS + VEGF vs. EBM + 5% FBS + VEGF	-643,6	-946,2 to -341,0	Yes	****
EBM + 2% FBS + VEGF vs. EBM + 10% FBS	-900,9	-1203 to -598,3	Yes	****
EBM + 2% FBS + VEGF vs. EBM + 10% FBS + VEGF	-1156	-1459 to -853,4	Yes	****
EBM + 2% FBS + VEGF vs. EGM-2	-1432	-1747 to -1117	Yes	****
EBM + 2% FBS + VEGF vs. EGM-2 + VEGF	-1672	-1987 to -1357	Yes	****
EBM + 5% FBS vs. EBM + 5% FBS + VEGF	-62,71	-365,3 to 239,9	No	ns
EBM + 5% FBS vs. EBM + 10% FBS	-320	-622,6 to -17,42	Yes	*
EBM + 5% FBS vs. EBM + 10% FBS + VEGF	-575,1	-877,7 to -272,6	Yes	****
EBM + 5% FBS vs. EGM-2	-851,5	-1166 to -536,6	Yes	****
EBM + 5% FBS vs. EGM-2 + VEGF	-1092	-1406 to -776,6	Yes	****
EBM + 5% FBS + VEGF vs. EBM + 10% FBS	-257,3	-559,9 to 45,30	No	ns
EBM + 5% FBS + VEGF vs. EBM + 10% FBS + VEGF	-512,4	-815,0 to -209,8	Yes	****
EBM + 5% FBS + VEGF vs. EGM-2	-788,8	-1104 to -473,9	Yes	****
EBM + 5% FBS + VEGF vs. EGM-2 + VEGF	-1029	-1344 to -713,9	Yes	****
EBM + 10% FBS vs. EBM + 10% FBS + VEGF	-255,1	-557,7 to 47,44	No	ns
EBM + 10% FBS vs. EGM-2	-531,5	-846,5 to -216,6	Yes	****
EBM + 10% FBS vs. EGM-2 + VEGF	-771,5	-1086 to -456,6	Yes	****
EBM + 10% FBS + VEGF vs. EGM-2	-276,4	-591,3 to 38,54	No	ns
EBM + 10% FBS + VEGF vs. EGM-2 + VEGF	-516,4	-831,3 to -201,5	Yes	****
EGM-2 vs. EGM-2 + VEGF	-240	-566,8 to 86,83	No	ns

8.1.4. Cell number vs PrestoPlue™ correlation at 48 hours

Table 6 – Tabular results of the statistical analysis of the correlation between cell number and PrestoBlue™ results at 48 hours.

	Cell Number vs.

	Fluorescence
Pearson r	
r	0,9487
95% confidence interval	0,8420 to 0,9840
R squared	0,9001
P value	
P (two-tailed)	< 0,0001
P value summary	****
Significant? (alpha = 0.05)	Yes
Number of XY Pairs	14

Table 7 – XY data of the statistical analysis of the correlation between cell number and PrestoBlue™ results at 48 hours.

	Cell Number	Fluorescence
EBM	349	704,4048
EBM + VEGF	881,7	1299,262
EBM + 0,1% FBS	664,7	1212,405
EBM + 0,1% FBS + VEGF	1220,3	1815,404
EBM + 1% FBS	1263,7	1923,976
EBM + 1% FBS + VEGF	1504,3	2514,262
EBM + 2% FBS	1726,3	2633,69
EBM + 2% FBS + VEGF	1792,7	2756,262
EBM + 5% FBS	1905,7	3337,118
EBM + 5% FBS + VEGF	1950	3399,833
EBM + 10% FBS	2021	3657,118
EBM + 10% FBS + VEGF	1910,7	3912,261
EGM-2	2028	4188,666